Report Cover Page

ACERA Project
1006b
Title
Model-based search strategies for plant diseases: a case-study using citrus canker (*Xanthomonas citri*)
Author(s) / Address(es)
Joanne M. Potts[1], Martin J. Cox[1], Rochelle Christian[2] and Mark A. Burgman[1] [1] Australian Centre of Excellence for Risk Analysis, The School of Botany, University of Melbourne, Victoria. [2] National Coordination Team, Department of Agriculture, Fisheries and Forestry, Canberra.
Material Type and Status (Internal draft, Final Technical or Project report, Manuscript, Manual, Software)
Final Report 4 (Stage 5)
Summary

The main aim of biosecurity response to an incursion is to achieve pest- or disease-free status as quickly as possible. One of the critical initial response activities involves tracing known movements (trace events) to and from an infected or infested property (IP) that could spread the pest or pathogen. During an incursion response, managers prioritize individual trace events, allocating surveillance resources to follow-up trace events in order of priority. Prioritizing trace events is difficult and typically subjective. We present a simulation model where different dispersal mechanisms spread a pest or pathogen between areas. We use model outputs to test different search strategies, using citrus canker (caused by the bacterium *Xanthomonas citri*) as a case study. Model scenarios are based on an outbreak of citrus canker that occurred in Emerald, Queensland, in 2004.

Model parameters were extracted from published scientific reports and elicited from experts. We used model outputs to assess four search strategies to determine how best to monitor citrus canker spread. Parameters governing disease detectability and host susceptibility were varied in a sensitivity analysis.

Flexible simulation software was implemented in program R. Whilst the simulator can be parameterised for many outbreak situations, no general rules can be established using the results of this study on citrus canker for tracing other pests or diseases: the simulator should be used on a case-by-case basis.

In all simulation scenarios, the “adaptive radius” rule performed best, whereby a circular search area was placed around the IP where the disease outbreak was first detected, with a radius proportional to the estimated number of months the property was infected. Importantly, none of the search rules tested detected all IPs without completely searching all properties with susceptible hosts in the region.

We identify a simple rule of thumb for searching during a citrus canker outbreak that is robust to uncertainty. No general rules can be established using the results of this study for tracing other pests or pathogens. The model has created a framework that may be used to explore other contexts and disease dynamics, leading perhaps to more general rules for disease outbreak management.

ACERA Use only	Received By:	Date:
	ACERA / AMSI SAC Approval:	Date:
	DAFF Endorsement: ( ) Yes ( ) No	Date:

Model-based search strategies for plant diseases: a case-study using citrus canker (*Xanthomonas citri*)

ACERA Project No. 1006b

Joanne M. Potts[1], Martin J. Cox[1], Rochelle Christian[2] and Mark A. Burgman[1]

1. Australian Centre of Excellence for Risk Analysis, The School of Botany, The University of Melbourne, Victoria.

2. National Coordination Team, Department of Agriculture, Fisheries and Forestry, Canberra.

Final Report 4 (Stage 5)

26th September 2012

Acknowledgements

This report is a product of the Australian Centre of Excellence for Risk Analysis (ACERA). In preparing this report, the authors acknowledge the financial and other support provided by the Australian Government Department of Agriculture, Fisheries and Forestry (DAFF), and the University of Melbourne.

We thank everyone on the reference group who provided us with invaluable insight into the biology of citrus canker and understanding trace priorities: Amy Forbes, Bruce Jackson, Chinatsu Yahata, Chris Adriaansen, Fiona MacBeth, Grant Telford, Karen Absolon, Karen Bailey, Lynn Broos, Marg Coonan-Jones, Mark Stanaway, Mike Ashton, Pat Barkley, Peter Whittle, Rob Baxter, Roger Paskin, Sama Low Choy, Sankham Hornby, Sharyn Taylor, Stephen Pratt, Tim Beattie, and Tony Monteith. Comments by Paul Pheloung, Chris Adriaansen, and two anonymous reviewers greatly improved the report.

Table of contents

Acknowledgements 2

Table of contents 3

List of Tables 5

List of Figures 6

1. Executive Summary 10

2. Introduction 11

3. Citrus canker 15

3.1. Species life history 15

3.2. History of outbreaks in the world and Australia 16

3.3. Economic importance 17

4. Model description 19

4.1. AOI definitions 20

4.2. Susceptibility 21

4.3. Disease progression and spread 23

4.4. AOI infectiousness 25

4.5. Dispersal Mechanisms 27

4.6. Anthropogenic dispersal mechanisms 27

4.7. Weather-based dispersal and establishment mechanisms 28

4.8. Disease detectability within an AOI 31

Citrus canker detectability within a host plant 31

4.9. Tracing 32

5. Simulation scenarios 35

6. Results 38

6.1. Summary Statistics 38

6.1. Tracing outputs 39

7. Discussion 46

7.1. Key findings 46

7.2. Implementation of model outputs for BioSIRT 46

7.3. Model performance and ideas for future research 47

7.4. Control measures 47

7.5. Cost 48

7.6. The spatial distribution of individual plants within an AOI 48

7.7. Wind dispersal model and other dispersal mechanisms 48

7.8. Severe storms 49

7.9. Influence of leafminer and mechanical wounds 49

7.10. AOI and host organism detectability 49

7.11. Future case studies? 50

7.12. Recommendations 50
7.13. Caveats 51
8. References 52
9. Appendix 1: Tree growth models 56
9.1. Model implementation information: tree area 56
10. Appendix 2: Example dispersion and establishment functions 58
10.1. Model implementation information: dispersal & establishment 58
10.2. Candidate dispersal and establishment functions 60

List of Tables

Table 1. History of outbreaks of citrus canker in Australia. [Source: Modified from Telford, O'Brien and Ashton (2009).]. 18

Table 2. Description of AOI types in the simulation model. Any number of AOI types can be described by the user (e.g. in some scenarios a “juicing factory” might be required). 21

Table 3. Dispersal mechanisms accounted for in this model. Any number of dispersal mechanisms can be defined by the user, some of which might be foreseeable for citrus canker dispersal, but not explicitly accounted for in our model (e.g., severe storms). Plots of example dispersal mechanisms are shown in Appendix 2. 30

Table 4. Examples of dispersal events from a single run of the simulation model.....38

List of Figures

Figure 1. Susceptibility of AOIs (i.e. probability of a target AOI becoming infected given that citrus canker inoculum has successfully dispersed to the target AOI) varies with temperature and tree age using a generalized beta function (Equation 1). The first element of the generalized beta function parameter vector, $\phi 1^*$, was modified to account for decreasing susceptibility with increasing tree age using Equation 2. In this figure, the curves progress from the most-susceptible, *a* = 0.1 year old trees, to least-susceptible trees with *a* ≥ 10. 23

Figure 2. Schematic of disease model dispersal and establishment structure. The contagious AOI is shown in red, with a list of AOI attributes. ‡ Duration infected is the time lapsed since infection of the contagious AOI. The model allows a time lag between an AOI being infected becoming contagious. †Fixed attributes can be varied with time, but this is not currently implemented. All dispersal and establishment parameters are shown in green, with the uninfected AOI in light blue. 24

Figure 3. Citrus tree canopy-area is modelled using a linear to 10 years old, and constant thereafter. The model has three different growth curves (Appendix 1) that can be determined by the user. 26

Figure 4. Variation in infectiousness after Dalla Pria *et al.* (2006). Left-hand panel: The effect of the number of rainfall hours on citrus canker infectiousness, represented as a scale coefficient, modelled using a monomolecular relationship: $\mathrm{hfft;b} = \mathrm{b1}[1\text{-}\mathrm{b2}\exp(\text{-}\mathrm{b3ft})]$, where b_1 = 1.168; b_2 = 0.15, and b_3 = 0.305. Right-hand panel: The effect of temperature on citrus canker infectiousness, represented as a scale coefficient. A generalized beta distribution was used, $\mathrm{gT(Tt;}\phi) = \phi 1^*[\mathrm{Tt}\text{-}\phi 2\phi 3(\phi 4\text{-}\mathrm{Tt})\phi 5]$, where ϕ_1 = 0.0264, ϕ_2 = 12.725; ϕ_3 = 1.465; ϕ_4 = 40.55, and ϕ_5 = 0.7575. 27

Figure 5. Probability of citrus canker detection in an infected AOI, $\mathrm{dt,C(t,C;}\theta\mathrm{,tI,thres})$, is dependent upon AOI infectiousness C, and time since infection, *t* (Equation 7). Curve plotted for parameters initial probability of detection θ_1= *3x10*$^{-4}$, and shape parameter θ_2 = *0.38*; $t_{I,thres}$ = *2*. 32

Figure 6. Example of probability of dispersal and establishment space. Matrix elements with a high Pr(disp) are red, low Pr(disp) blue. In this example, the vertical line at AOI number 59 (a commercial nursery) represents different dispersal and establishment mechanisms from the nursery to citrus farm vs. citrus farm to commercial nursery. 34

Figure 7. Map of hypothetical citrus-growing region (based on Emerald, Queensland), with areas of citrus trees represented as a network of AOIs. Each AOI (solid black dot) is defined by a spatial location and area, and contains a number of citrus plants, with a mean-tree age. Areas shaded dark orange and yellow are commercial citrus growing areas, and properties that contain commercial citrus areas, respectively. ...36

Figure 8. Weekly time series of weather data (x-axis weeks from 1 Jan), and modelled AOI attribute values. First row panels show weekly rainfall duration and temperature from the Australian Bureau of Meteorology for Emerald, QLD (black line) and Mildura, VIC (grey line). Model results are shown in rows two and three: Infectiousness is calculated for an AOI containing 1,000 2-year old trees. Dispersal probability is dependent upon infectiousness, and duration of infection. Establishment probability is based upon citrus variety, mean tree age and temperature. Detection probability is proportional to ln(infectiousness). 37

Figure 9. As time progresses in the simulations since time of true day 0 (x- axis), the number of AOIs infected that are detected increases non-linearly with respect to time. 39

Figure 10. Trace method performance using Emerald region spatial data with dispersal and establishment parameter set based on (A) Emerald and (B) Mildura weather data (c.f. Figure 8). Probability of detecting citrus canker at an infected AOI was 1.0. Trace strategies colour coded, with points showing mean performance annotated by strategy-type search criteria: search radii for adaptive radius; number of nodes searched for closest n nodes, probability space and ranked probability searches. Ribbons are the +/- 2 standard errors calculated from 1,000 simulations (see Section 3). 41

Figure 11. Trace method performance using Emerald region spatial data with dispersal and establishment parameter set based on (A) Emerald and (B) Mildura weather data (c.f. Figure 8). Probability of detecting citrus canker at an infected AOI was 0.9. Trace strategies colour coded, with points showing mean performance annotated by strategy-type search criteria: search radii for adaptive radius; number of nodes searched for closest n nodes, probability space and ranked probability searches. Ribbons are the +/- 2 standard errors calculated from 1,000 simulations (see Section 3). 42

Figure 12. Trace method performance using Emerald region spatial data with dispersal and establishment parameter set based on (A) Emerald and (B) Mildura weather data (c.f. Figure 8). Probability of detecting citrus canker at an infected AOI was 0.7. Trace strategies colour coded, with points showing mean performance annotated by strategy-type search criteria: search radii for adaptive radius; number of nodes searched for closest n nodes, probability space and ranked probability searches. Ribbons are the +/- 2 standard errors calculated from 1,000 simulations (see Section 3). 43

Figure 13. Trace method performance using Emerald region spatial data with dispersal and establishment parameter set based on (A) Emerald and (B) Mildura weather data (c.f. Figure 8). Probability of detecting citrus canker at an infected AOI was 0.5. Trace strategies colour coded, with points showing mean performance annotated by strategy-type search criteria: search radii for adaptive radius; number of nodes searched for closest n nodes, probability space and ranked probability

searches. Ribbons are the +/- 2 standard errors calculated from 1,000 simulations (see Section 3). 44

Figure 14. Trace method performance using Emerald region spatial data with dispersal and establishment parameter set based on (A) Emerald and (B) Mildura weather data (c.f. Figure 8). Probability of detecting citrus canker at an infected AOI was 0.3. Trace strategies colour coded, with points showing mean performance annotated by strategy-type search criteria: search radii for adaptive radius; number of nodes searched for closest n nodes, probability space and ranked probability searches. Ribbons are the +/- 2 standard errors calculated from 1,000 simulations (see Section 3). 45

1. Executive Summary

The main aim of biosecurity response to an incursion is to achieve pest- or disease-free status as quickly as possible. One of the critical initial response activities involves tracing known movements (trace events) to and from an infected or infested property (IP) that could spread the pest or pathogen. During an incursion response, managers prioritize individual trace events, allocating surveillance resources to follow-up trace events in order of priority. Prioritizing trace events is difficult and typically subjective. We present a simulation model where different dispersal mechanisms spread a pest or pathogen between areas. We use model outputs to test different search strategies, using citrus canker (caused by the bacterium *Xanthomonas citri*) as a case study. Model scenarios are based on an outbreak of citrus canker that occurred in Emerald, Queensland, in 2004.

Model parameters were extracted from published scientific reports and elicited from experts. We used model outputs to assess three search strategies to determine how best to monitor citrus canker spread. Parameters governing disease detectability and host susceptibility were varied in a sensitivity analysis.

Flexible simulation software was implemented in program R. Whilst the simulator can be parameterised for many outbreak situations, no general rules can be established using the results of this study on citrus canker for tracing other pests or diseases: the simulator should be used on a case-by-case basis.

In all simulation scenarios, the “adaptive radius” rule performed best, whereby a circular search area was placed around the IP where the disease outbreak was first detected, with a radius proportional to the estimated number of months the property was infected. Importantly, none of the search rules tested detected all IPs without completely searching all properties with susceptible hosts in the region.

We identify a simple rule of thumb for searching during a citrus canker outbreak that is robust to uncertainty. No general rules can be established using the results of this study for tracing other pests or pathogens. The model has created a framework that may be used to explore other contexts and disease dynamics, leading perhaps to more general rules for disease outbreak management.

2. Introduction

Pest or pathogen (hereafter, referred to as a pest) dispersal is a complex process, whereby non-infected areas may be exposed to a pest via numerous pathways, which may be human-assisted (e.g., movement of infected or infested material) or natural (e.g., wind). Increasing the frequency of dispersal mechanisms between an infected area and a non-infected area increases exposure to the pathogen (Gertzen *et al.* 2011). Importantly, exposure does not guarantee infection, which is a process affected by many chance events such as whether environmental conditions favour survival of the pest, or if the host species is present in the exposed area and in a receptive state to the pest.

During an incursion response, managers need to determine rapidly the extent of the incursion by inspecting exposed areas (Mangano 2011). Exposure pathways are any means that allows the entry or spread of a pest and include ‘trace events’ (i.e., known movements of items such as animals, personnel, vehicles and equipment that may potentially spread the pest, Patyk *et al.* 2011) and other potential dispersal mechanisms (e.g., wind). The term ‘day 0’ is given to the estimated date of initial infection. Movements along exposure pathways are directional. ‘Forward’ movements are away from an infected area, occurring since day 0 that may have spread the pest to other areas. ‘Backward’ movements are to the infected area, occurring prior to day 0 that may have introduced the pest. Exposure pathways link potentially infectious areas. Response managers inspect these potentially exposed areas and when they find additional infected areas, they take appropriate actions (e.g., destroy all infected host species), aiming to eradicate the disease as quickly as possible (Keeling 2005).

To allocate resources efficiently, emergency response managers set priorities for following up trace events (called “trace priorities”), such that areas with high probability of having the pest are given a higher priority and inspected for disease before lower priority areas (Hagerman 2010). Other potential, but unknown movement of items along exposure pathways, may also be followed-up where they expose susceptible hosts to the pest.

The reliance on domain experts to rank individual trace events is controversial, as experts may be influenced by a range of contextual and subjective factors external to a specific outbreak (Slovic, 1999; Perry *et al.*, 2001). Often judgements of risk—like those that inform the prioritisation of traces in an emergency response—are not only based on technical analysis, but on intuitive reactions and political judgements (Wilkinson *et al.* 2011). For example, the closure of all rural footpaths during an outbreak of foot and mouth disease (FMD) in Britain in 2001 is now considered draconian and reflected a perceived risk of recreational walkers spreading FMD rather than a real risk. Footpath closures ended up

costing more money to the tourist industry than the actual cost to agriculture of the FMD outbreak (Wilkinson *et al.* 2011). Therefore, there is a clear need "for scientists to provide robust tools" that support "effective participation in disease management" (Wilkinson *et al.* 2011, p. 1939).

Increasingly, models are being used to simulate disease dispersal and investigate aspects that different management actions have, for example, on the cost of eradication, or assessing the timeframe or likelihood of successful eradication given different management actions (e.g., Dybiec *et al*. 2005). Such models may be deterministic and useful for understanding basic infection dynamics but have limited predictive ability, since any one epidemic is unlikely to follow an 'average pattern' (Garner and Hamilton 2011); or stochastic, where natural variability and uncertainty in the input parameters is accommodated (Garner and Hamilton, 2011). Consequently, each time a stochastic model is run, the result is different (as would be any two outbreaks of a disease in real life). Summary statistics such as the mean, range and variance of results are used to represent the output of the system from many iterations of the model. Stochastic models are more complicated to construct, but are particularly useful for assessing risks and can be used to investigate the likelihood of different outcomes (Garner and Hamilton, 2011).

Most applications of models to investigate spread have focused on animal and human diseases. For example, AusSpread, is a stochastic, state transition susceptible-latent-infected-recovered (SLIR) model, that can be used to simulate scenarios for policy planning, vulnerability analysis and decision-making (Garner and Beckett, 2005). Using AusSpread, the effectiveness of various control strategies can be investigated under different environmental conditions that govern how FMD spreads. AusSpread incorporates traces by modeling the probability of detecting an infected farm based on whether that farm had contact (direct or indirect) with a farm with known infection (Garner and Beckett, 2005). The system's sensitivity (proportion of AOIs correctly identified as dangerous contacts) and specificity (proportion of AOIs incorrectly identified as dangerous contacts) can be estimated.

The North American Animal Disease Spread Model (NAADSM) is a stochastic, simulation based model that has been used to guide policy decisions to a variety of animal diseases including FMD, Aujezsky's disease and avian influenza (Reeves *et al.* 2011). Similarly, InterSpread (www.interspreadplus.com) has been used to investigate the outbreak of FMD in New Zealand. Similar studies have been undertaken for human diseases (e.g., small pox, Ferguson *et al.* 2003). Although these models allow user-defined priorities for which AOI to visit (i.e., trace priorities), as far as we are aware these systems have not been used to evaluate choice of tracing rule sets.

Models such as AusSpread, NAADSM and InterSpread show that disease and pest dispersal is complex. Complex models have an intuitive appeal because they are frequently considered more accurate. But a model is only as good as the data that are used to parameterize it, and complex models require more information (Keeling 2005). Models cannot replicate a host of subtle details and local information used by experts to develop trace priorities (Keeling 2005), but can provide an assessment of general sets of risk-based trace priorities in a transparent, explicit and accountable manner.

There are fewer applications of models to address disease spread within the plant health sector (Jeger *et al.* 2007), and such examples are typically generated as complex, single solutions and lack the general framework to develop rules for searching across a range of scenarios. One example is Fox *et al.* (2009) who investigated surveillance protocols for Chilean needle grass (*Nassella neesiana*). This model was developed using Python in ArcGIS software (Fox *et al.* 2009). Cacho *et al.* (2010) developed a spatially-explicit model to investigate the importance of passive surveillance in eradication success, and these theoretical results could be applied to plant species. The animal health sector benefits by sometimes having extensive data sets obtained from censuses and systems for tracking livestock (Garner and Beckett, 2005). Also, pest incursions in the plant health sector might be considered more challenging since typically:

1. the time lag between when the pest or disease was introduced until the time it is detected can be long (in some cases, years). Therefore, the uncertainty in estimating day 0 is greater for pests of concern to the plant health sector than for the animal health sector, and
2. host species and habitats, and their distributions, are not known with certainty.

These issues create three complications for modeling pests of plants. Firstly, if the estimate of day 0 is uncertain, the trace priorities will likewise be uncertain. Secondly, there is typically incomplete knowledge regarding movement events. This includes the timing of movement events (e.g., a property owner declared a movement event occurred but the date was uncertain), whether the events actually occurred (e.g., a weather event capable of pest dispersal was recorded in the region but it is unknown if it directly affected the IP, or the movement of wild host animals on to and away from an infected property), and the implications of the type of movement for the probability of pest spread (e.g., some movement events may pose greater probability of disease spread than others and the probability of spread may be uncertain). In addition, multiple movement events might occur between a source AOI and a destination AOI, leading to increased risk of disease spread, if only one such movement event had occurred.

Thirdly, since host species and habitats might not uncertain, infected but unknown host populations may act as a source for re-infection, making eradication attempts futile. For example, citrus canker is a bacterial disease of plants in the Rutaceae family caused by *Xanthomonas citri* (Hasse) Vauterin. In Australia, the location of some host species may be known (e.g., commercial citrus grown in orchards), while others are not (e.g., citrus trees grown in backyards, or the distribution of the native host *Citrus glauca* in bushland).

We aim to develop general search strategies for use in plant health emergencies. We present a spatially-explicit, stochastic, state-transition model, where disease spread occurs between susceptible populations. The model generally follows the structure and conventions developed by Garner and Beckett (2005). Disease spread occurs via different mechanisms (e.g., wind dispersal or the movement of diseased plant material), that include, but are not limited to, known movements of items between two AOIs. Various rule sets to rank traces are investigated via a simulation study, to determine how best to contain disease spread. We parameterise the model using citrus canker (*Xanthomonas citri*) as a case study.

Citrus canker is a plant-pathogenic bacterium that causes lesions on leaves, shoots, branches and fruit of several susceptible species within the Rutaceae family (Goto 1992, Gottwald *et al.* 2002). Three forms of citrus canker disease are differentiated mainly by their geographical distribution and host range (Das 2003). We focus on the Asiatic form of canker (*X. citri* (Hasse) Vauterin), which is the most common, widespread and severe form of the disease (Das 2003). It was also this form of the bacteria that was responsible for the outbreak of citrus canker in Emerald, Queensland in July 2004 (Gambley *et al.* 2009).

3. Citrus canker

3.1. Species life history

Citrus canker thrives in warm, humid climates (Das 2003). The bacterium persists as epiphytes on the plant surface before entering susceptible plant tissue. Typically, for infection to occur the bacterial cells must impact susceptible plant tissue with enough force to penetrate the stomatal aperture (e.g., during high wind events, with wind speeds greater than 8m/s, Gottwald and Irey 2007), or enter susceptible plant tissue via wounds caused by mechanical damage (e.g., branch fall, pruning) or injury caused by insects (e.g., leaf miner, Gottwald *et al.* 2002, Gottwald and Irey 2007, Gottwald *et al.* 2007, Hall *et al.* 2010, Jesus *et al.* 2006). Plants are most susceptible to stomatal infection through expanding (50-80% fully expanded) leaf tissues, where growth occurs in several well-defined waves (or flushes) during the growing season (Koizumi 1981; Graham *et al.* 2004). The number of flushes occurring annually depends on the variety of citrus, and climatic conditions (under cool climatic conditions only two flushes appear annually while 3-5 flushes occur in warmer subtropical regions, Spiegel-Roy and Goldschmidt 1996). Immature fruit is most susceptible to infection from just after petal-fall through the period of fruit enlargement (Stall *et al.* 1980).

In optimal conditions, only 1-2 bacterial cells are required to colonise a host plant (Graham *et al.* 2004). The bacteria multiply and large numbers of bacterial cells create lesions on the surface of the leaves, stems and fruit of the host plant. The number of bacteria cells inside of lesions are correlated with lesion size and age. As lesions grow and disease intensifies, defoliation occurs. The time frame between initial infection and defoliation depends on the susceptibility of the host species. When wet, the lesions may begin to ooze bacteria from stomatal pores five days after infection, providing inoculum for further infection. The earliest visual symptoms on leaves appear around 7-10 days post-infection (Graham *et al.* 2004, Gottwald *et al.* 1989). Under adverse conditions, lesions may take up to 60 days to appear (Gottwald and Graham 1992, Dalla Pria *et al.* 2006). Symptoms vary depending on susceptibility of host species (e.g.., grapefruits are more susceptible, Graham *et al.* 2004), and the plant tissue and timing of infection (e.g., symptoms of late infections of wounded fruits are atypical; Koizumi, 1974).

In the presence of suitable rainfall events, temperature ranges between 20 to 30^{o}C are considered optimal conditions for citrus canker bacteria (Bock *et al.* 2005), but the bacteria can survive between 12 to 40^{o}C (Dalla Pria *et al.* 2006). Typically, no bacteria survive in temperatures greater than 42^{o}C (Dalla Pria *et al.* 2006), and cooler temperatures in winter reduce the number of bacteria (Bock *et al.* 2005).

Bacteria that ooze onto plant surfaces die within hours from exposure to direct sunlight. Bacteria may survive, if sheltered from direct sunlight, on various inanimate surfaces such as metal, plastics, cloth and processed wood for up to 72 hours (Graham *et al.* 2000, Das 2003). This implies dispersal of canker bacteria can occur via machinery and infected equipment (e.g., pruners, hedge trimmers, picking bags, clippers) if used immediately and not cleaned before re-use, contributing to spread of citrus canker within citrus trees and within orchard blocks. However, dispersal between orchard blocks via contaminated equipment and machinery is less likely (but still possible) since the bacteria are likely to die due to exposure, unless citrus blocks are neighbouring, and contaminated equipment is used immediately and not cleaned before re-use. If contaminated equipment, such as picking bags or clothing remained damp, survival of the citrus canker bacteria might be longer.

Citrus canker bacteria may survive a few days in soil, or a few months in plant material in soil. Once diseased leaves and fruit drop to the ground, bacteria are typically not detectable within 1-2 months, depending on environmental conditions (Graham *et al.* 2004). Time since infection can be estimated based on lesion size and location on the host plant in horticultural settings, but it is harder to estimate time since infection in residential settings because of the lack of routine plant care (Graham *et al.* 2004).

3.2. History of outbreaks in the world and Australia

Citrus canker is believed to be endemic to India, Pakistan, islands of the Indian Ocean, China, Japan and other south-east Asian countries, from where it has spread to other citrus growing continents with the exception of Europe (Das 2003). Citrus canker has been detected at various times in the Gulf States region of USA, South America, South Africa, Saudi Arabia, New Zealand and Australia since the early 1900s (Das 2003), with varying eradication campaigns that have been successful (e.g., Australia) or not (e.g., Florida, USA). The history of outbreaks in Australia is summarised in Table 1, with the most recent outbreak occurring in Emerald, Queensland in 2004.

The entry mechanism in the outbreak in Emerald is uncertain. Mechanisms of short-distance disease spread within blocks were identified as wind-driven rain and movement of contaminated farm equipment (in particular pivot irrigator towers via mechanical damage in combination with abundant water, Gambley *et al.* 2009). Medium-distance dispersal between infected properties in Emerald was attributed to movement of contaminated farm equipment and/or people and storm events (Gambley *et al.* 2009). No evidence was found for long-distance dispersal from infected properties in Emerald to other regions.

Other outbreaks of citrus canker have been declared 'ineradicable'. For example, government agencies attempted citrus canker eradication for years in Florida, prior to several severe storms that dispersed citrus canker inoculum across large areas (Irey *et al.* 2006). Consequently citrus canker was declared "ineradicable" in Florida in January 2006 (Gottwald and Irey, 2007). Citrus canker is also now considered endemic in South America.

3.3. Economic importance

If citrus canker infects fruit during their early growing period, the fruits crack or become malformed as they grow and heavily infected fruits fall prematurely (Gottwald *et al.* 2002; Das 2003). Light infection of fruit in later growth stages may cause only scattered canker lesions on the surface of fruit, but the blemishes are unsightly, rendering the fruit unacceptable for market (Das 2003). Since the detection of citrus canker triggers immediate quarantine restrictions and disrupts the movement of fresh fruit, the economic impact of lost markets is actually much greater than that from reductions in the yield and quality of the crop (Graham *et al.* 2004). Consequently, worldwide, millions of dollars are spent annually on prevention, quarantine, eradication programs and disease control (Das 2003).

The eradication campaign in Emerald involved the destruction of all host plants within the Emerald area, with the exception of *Citrus glauca*, a native species, which was widespread. Instead, *C. glauca* was eradicated near commercial premises only. The eradication campaign was completed in 2009, and the cost was estimated at $17.6 million dollars (Gambley *et al.* 2009); but this estimate does not include the cost to the industry (Alam and Rolfe 2006).

249 **Table 1. History of outbreaks of citrus canker in Australia. [Source: Modified from**
250 **Telford, O'Brien and Ashton (2009).].**
251

Year	Summary of incident
1912	Detected in lime and lemon trees at Milton Homestead, Stapleton and at Port Darwin, NT.
1916	Two consignments of fruit from Japan and China found infected with canker in Sydney. Citrus trees at Stapleton and Darwin Botanic Gardens destroyed.
1918	Citrus canker detected in Darwin, Penpelli, Stapleton and at Daly River Settlement.
1922	New outbreaks of citrus canker discovered in Darwin, including Pine Creek, and eradicated.
1981	Citrus canker detected in the Cocos (Keeling) Islands and eradicated.
1984	Citrus canker detected on Thursday Island and eradicated.
1991	Citrus canker found in Lambells Lagoon, NT.
1993	Further infected trees found at Lambells Lagoon. Eradicated.
2004	Citrus canker found in Emerald, Queensland. Canker reported on a citrus /grape orchard at Emerald July 2004; found on 2nd property October 2004; on 3rd property May 2005; all hosts eradicated December 2005; declared eradicated February 2009.

4. Model description

We present a computer simulation model that is based on graph-theory, in which there are numerous nodes representing AOIs, each with different properties, in a region. Our definition of an AOI is a geographic area comprising a point, line or polygon on a map that contains susceptible hosts or possible habitats, or that may act as a conduit for pest dispersal, e.g., packing shed. Our rational for using a computer simulation model was:

(i) In the simulation model, the truth is known: it is known where initial infection(s) occurred within the geographical area of interest (AOI), and which dispersal mechanisms are responsible for disease spread and to which AOIs, providing a platform to consolidate data and understand the ecology of the pest and its hosts. This is different to a real outbreak of a pest or disease, where often the source of the outbreak, or where and how it has spread, are unknown;

(ii) Expert knowledge about model parameters, including uncertainty, can be incorporated into simulations; and

(iii) The model can be used to test the efficacy of alternative trace protocols.

We use discrete, weekly, time-steps. At each simulation time-step, several processes may affect individual nodes (Harvey *et al.* 2007). In any time step, a proportion of AOIs will be infected, and the disease status of these AOIs will be known (i.e., whether the disease is present and is readily detectable) or unknown (i.e., whether the disease is present and undetectable, or the disease is absent).

Infected AOIs are connected to other AOIs by different dispersal and establishment mechanisms (‘exposure pathways’ where for the purposes of our model these include, but are not limited to, known trace events or the movements of items). Two AOIs might be connected by multiple dispersal mechanisms. The model we present explicitly accumulates the risk of disease spread for AOIs that are highly connected. Dispersal and establishment mechanisms are dependent on the activities which take place at an AOI and are ‘AOI-type’ to ‘AOI-type’ specific, and can be directional e.g. dispersal mechanisms from AOI type 1 to AOI type 2 can be defined differently to dispersal mechanisms from AOI type 2 to AOI type 1.

In our model, not all AOIs on the network must be known. That is, AOIs with susceptible hosts can exist, receive the disease and spread the disease, until these AOIs are discovered via surveillance. This is different to many models of disease spread in animals, which typically assume all AOIs in the network are known (e.g., Garner *et al.* 2011).

285 ### 4.1. AOI definitions

286 As noted above, in this model, an AOI represents a group of susceptible hosts or possible
287 habitats spatially clustered together (e.g., an orchard), or that may act as a conduit for
288 disease or pest dispersal (e.g., a packing shed). For the citrus canker simulation study, we
289 define seven 'AOI types'. There can be many AOIs of each AOI type within the simulation
290 study region. Each AOI comprises a unique spatial location that is defined by: the area of the
291 AOI, the number of susceptible host plants, the variety of susceptible host plants, and the
292 mean age of host plants within an AOI. Susceptibility of host plants can change with
293 weather-related conditions (see Section 3.2). We assume treatment of individual host plants
294 within an AOI is consistent and as such, an AOI within a commercial setting can be
295 considered equivalent to a "block" of citrus. We take a citrus block to be a contiguous area
296 with the same citrus species.

297 Host plants within an AOI age during the simulation. Movement of plant material between
298 AOIs is implicitly considered in the dispersal and establishment mechanisms, and how the
299 infectiousness of AOIs changes over time. As with other dispersal and establishment
300 pathways, dispersal and establishment arising from movement of plant material can be
301 traced within the simulation. If uninfected, an AOI is susceptible to infection (Section 3.2). If
302 infected, an AOI can disperse inoculum to uninfected AOIs (Section 3.3).

303 Any number of AOI types (e.g., Table 2) can be defined, the only restriction being that the
304 dispersal and establishment mechanisms must be defined for each new AOI type, a process
305 that may be restricted by data availability.

306

307

Table 2. Description of AOI types in the simulation model. Any number of AOI types can be described by the user (e.g. in some scenarios a "juicing factory" might be required).

Node	Description
Citrus block	Block of many hundreds or thousands of citrus trees within a commercial setting, primarily for production of fruit or condiment leaves (e.g., kaffir lime). Each is a contiguous area within which a single citrus species is grown.
Packing shed	Where citrus fruit is packed, ready for shipping.
Commercial nursery	Where citrus material is propagated for planting in citrus blocks or shipping to retail nurseries.
Retail nursery	Where citrus material is propagated and dispersed to backyards.
Private nursery	Where citrus material is propagated and dispersed to backyards e.g. farmers markets (i.e. less regulated than commercial and retail nurseries).
Native	Wild growing populations of native susceptible species (e.g., *Citrus glauca*) in e.g. national parks and reserves represented as a single node with many native plants.
Backyard	Individual citrus trees in backyard settings.

4.2. Susceptibility

An AOI must be susceptible to dispersing inoculum in order to become infected. That is, there must be suitable habitats or host plants at the destination node for the pathogen to establish there, and host plants must be in a growth-stage that is susceptible to infection and environmental conditions must be conducive. The user can specify the relationship between node susceptibility and the number of host plants at the node, their size and growth stage. The susceptibility of plants within an AOI to citrus canker increases with the number of flushes the plant experiences, citrus fruit variety and when plants are damaged. Susceptibility of the receiving node, g_s, Equation 1, was modified by temperature in a given time step, T_t, and mean tree age, a_i at the *i*th node. The probability of establishment is

related to temperature by a generalized beta relationship between inoculum load and temperature, following Dalla Pria *et al.* (2006):

$$\boldsymbol{g_s(T_t, a_i; \phi) = \phi_1^*[(T_t - \phi_2)^{\phi_3}(\phi_4 - T_t)^{\phi_5}]} \qquad \text{Equation 1}$$

where ϕ is a vector of parameters $(\phi_1^*, \phi_2, \ldots, \phi_5)$. Citrus trees grow in flushes, where new growth tissue is more susceptible to citrus canker infection. Older citrus trees typically experience fewer growth flushes, so ϕ_1 in Dalla Pria *et al.* (2006) was modified until plants reached 10 years in age, a_{max}, by:

$$\boldsymbol{\phi_1^* = \begin{cases} \phi_1 - a/2000 \ with\ 0 < a \leq a_{max} \\ \phi_1 - a_{max}/2000 \ with\ a > a_{max} \end{cases}} \qquad \text{Equation 2}$$

where ϕ_1^* is ϕ_1 adjusted for age. Other parameters in Equation 1 were obtained from Dalla Pria *et al.* (2006): $\phi_1 = 0.0264$, $\phi_2 = 12.725$; $\phi_3 = 1.465$; $\phi_4 = 40.55$, and $\phi_5 = 0.7575$).

We scaled the generalized beta relationship to represent AOI susceptibility as temperature- and host-age dependent, so that the curve maximum was equal to one, and used this curve to represent AOI susceptibility, based on temperature and mean tree age of the target AOI (Figure 1). The influence of citrus species or variety, *V*, upon an AOI's susceptibility can be modelled by applying a multiplication factor, k_V, to the susceptibility function $g_s(T_t, a; \boldsymbol{\phi})$. So the citrus variety-specific susceptibility of AOIs can be modelled by $g_{s,V}(T_t, a, k_V; \boldsymbol{\phi}) = g_s(T_t, a; \boldsymbol{\phi}) \times k_V$.

Increases in susceptibility arising from tree damage caused by movement of machinery or pruning were modelled implicitly within the dispersal kernels: in these cases, the probability of dispersal and establishment includes increases in susceptibility caused by damage to a number trees within an AOI (also see Discussion).

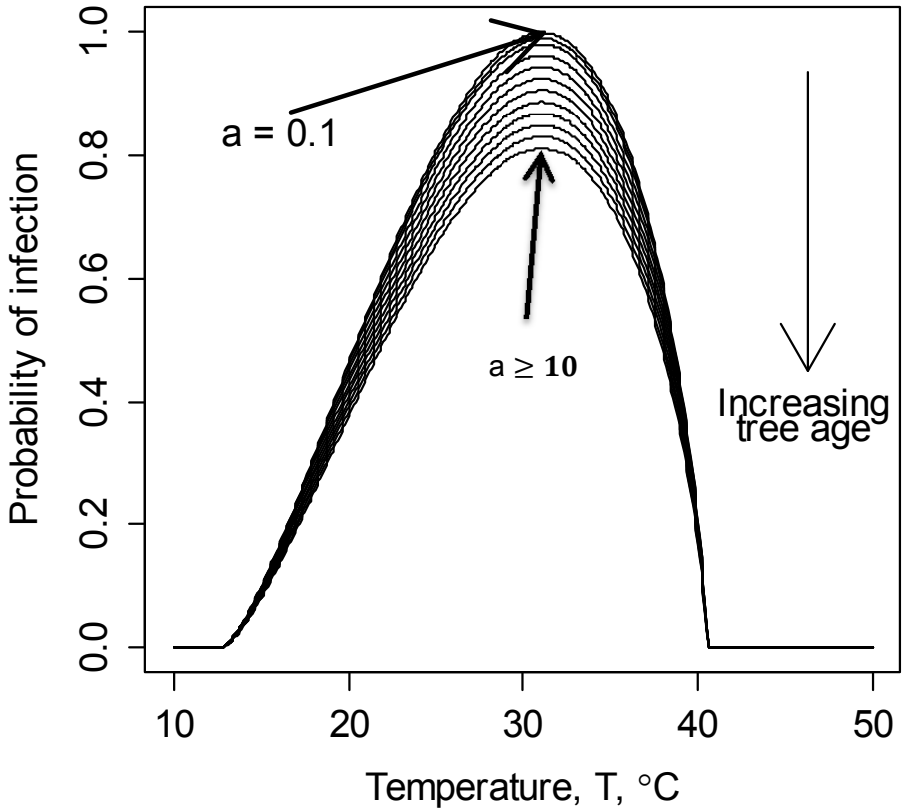

Figure 1. Susceptibility of AOIs (i.e. probability of a target AOI becoming infected given that citrus canker inoculum has successfully dispersed to the target AOI) varies with temperature and tree age using a generalized beta function (Equation 1). The first element of the generalized beta function parameter vector, ϕ_1^*, was modified to account for decreasing susceptibility with increasing tree age using Equation 2. In this figure, the curves progress from the most-susceptible, *a* = 0.1 year old trees, to least-susceptible trees with *a* ≥ 10.

4.3. Disease progression and spread

Infected AOIs become contagious after a specified period of incubation (Figure 2~~Figure 2~~). The incubation period may be zero weeks in duration, in which case nodes are infectious in the next time step after becoming infected. Once contagious, AOIs may infect other disease-free, susceptible AOIs. Within the model, three processes must occur for the infection to spread:

1. Firstly, there must be a sufficient amount of disease inoculum present within the contagious node before the risk of disease spread to other uninfected nodes is appreciable (i.e., although in theory it takes a single bacterium to spread and create another infection, this is unlikely). An AOI's infectiousness is calculated per time step and is determined by the number of trees in an AOI, mean age of trees in an AOI, and can vary with weather (see section 3.4 for infectiousness).
2. Secondly, one or more movement event/s must occur to transport the inoculum between the contagious node and the receiving node. Movement events (or dispersal mechanisms) can be described by a variety of smooth functions, based on AOI-edge to AOI-edge distance and angle (relative to the wind direction) between the source

and destination AOIs, or simple Bernoulli trials (see section 4.5 for Dispersal Mechanisms). Parameters within each dispersal mechanism can vary with time.

3. Thirdly, the destination AOI must be in a state susceptible to infection (see previous section).

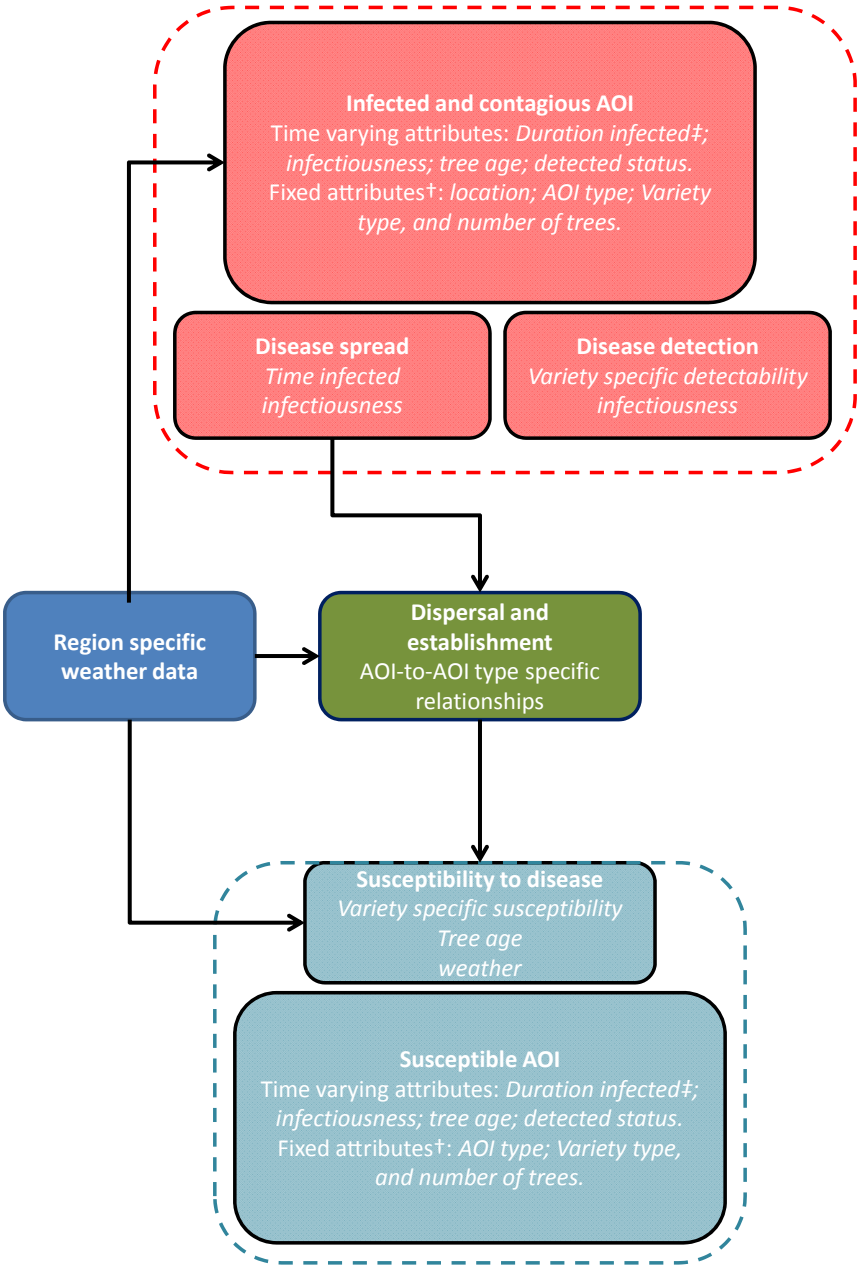

Figure 2. Schematic of disease model dispersal and establishment structure. The contagious AOI is shown in red, with a list of AOI attributes. ‡ Duration infected is the time lapsed since infection of the contagious AOI. The model allows a time lag between an AOI being infected becoming contagious. †Fixed attributes can be varied with time, but this is not currently implemented. All dispersal and establishment parameters are shown in green, with the uninfected AOI in light blue.

4.4. AOI infectiousness

When lesions are wet during rain events, they ooze citrus canker bacteria that enter rain droplets and can readily be wind dispersed. Wind speeds >8 m/s are strong enough to drive rain droplets into stomatal pores and create further infections (Gottwald and Irey 2007). Rainfall, temperature, wind speed and wind direction are explicitly considered in our model. We implicitly account for the interactions between environmentally-driven dispersal mechanisms by using observed weather data for each of the study areas. At each simulation time step, wind speed and wind direction dispersal mechanisms are included by re-parameterizing dispersal mechanisms using weather data records.

We model the effect of temperature and rainfall on citrus canker dispersal using the concept of citrus canker infectiousness (as defined in section 4.3 above). The idea behind using infectiousness is that we can base the probability of citrus canker dispersing and establishing from an infected AOI by taking into account both the citrus host plant characteristics (e.g., mean-tree age) at an infected AOI and weather events. At each time step within the simulation, we track the level of infectiousness at every infected AOI. When initially infected, the number of host trees and mean-tree age within the AOI determines AOI infectiousness. At subsequent time steps, we model variation in infectiousness using the relationships between citrus canker lesion density and temperature and rainfall obtained from Dalla Pria *et al.* (2006). Once infected, infectiousness will also vary with the time of infection.

The probability of dispersal from a contagious AOI to a susceptible AOI is, in part, proportional to the contagious AOI's infectiousness. The host plant size and architecture, age of lesions, severity of infection, rainfall intensity, wind speed and nature of the rain splash affect the quantity of bacteria dispersed and could explain much of the difference in numbers of bacteria dispersed in different experimental studies (Bock *et al.* 2005). Therefore, instead of using exact inoculum load in each contagious AOI, we use a relative measure: 'infectiousness', C_i. For AOIs that contain trees (e.g., citrus blocks), the infectiousness represents variation in dispersal, proportional to the total citrus tree basal area, mean tree age, rainfall and temperature. Upon initial infection, we model infectiousness in the *i*th node as:

$$\boldsymbol{C_i(A_{bi}, a_i, n_i) = \ln(n_i)\ \frac{A_{bi}}{a_i}} \qquad \text{Equation 3}$$

where, A_{bi} is total citrus tree canopy area within an AOI *i*, a_i is mean tree age and n_i is the number of trees within AOI *i*. The above formulation was based on expert opinion, and ignores the effect of rainfall and temperature on infectiousness. Equation 3 is only used when citrus canker is established within an AOI for the first time, or during re-establishment

after environmental conditions destroyed all inoculum within an infected AOI (e.g., temperatures greater than 42°C, Dalla Pria *et al.* 2006). We modelled tree canopy area as linear growth to a fixed age (10 years), and constant thereafter (Figure 3~~Figure 3~~).

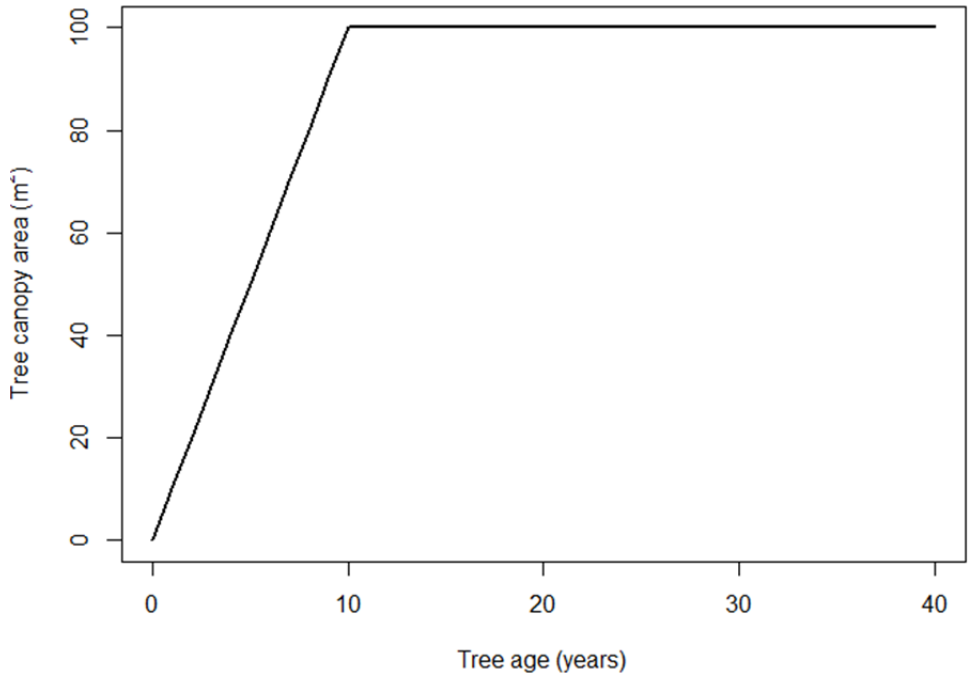

Figure 3. Citrus tree canopy-area is modelled using a linear to 10 years old, and constant thereafter. The model has three different growth curves (Appendix 1) that can be determined by the user.

After the initial infection, or re-establishment of citrus canker, a multiplicative function is used to model infectiousness. Infectiousness within the current time step *t*, at AOI *i*, depends on infectiousness in the previous time step *t-1*. Following Dalla Pria *et al.* (2006) infectiousness also depends on temperature, T_t, and the number of rainfall hours per week, f_t, by including a multiplicative index of inoculum load, at time *t*, giving:

$$\mathbf{C}_{i,t}(\mathbf{T}_t, \mathbf{f}_t; \boldsymbol{\phi}, \mathbf{b}) = \mathbf{C}_{i,t-1} \times \mathbf{g}_T(\mathbf{T}_t; \boldsymbol{\phi}) \times \mathbf{h}_f(\mathbf{f}_t; \mathbf{b}) \qquad \text{Equation 4}$$

A function describing the relationship between the number of hours of rainfall per week, and infectiousness, $h_f(f_t; \boldsymbol{b}) = b_1[1 - b_2\exp(-b_3 f_t)]$, was used with parameters obtained from mean values in Dalla Pria *et al.* (2006) b_1 = 1.168; b_2 = 0.15, and b_3 = 0.305 (see Figure 4~~Figure 4~~).

The function describing the effect of temperature on infectiousness, $g_T(T_t; \boldsymbol{\phi})$, is a normalised generalized beta function, with parameter vector, φ, between the minimum, $\boldsymbol{\phi}_2$, and maximum,$\boldsymbol{\phi}_4$, temperatures within which citrus canker bacteria can survive:

$$\mathbf{g_T(T_t;\phi)} = \begin{cases} \mathbf{0} \quad \mathbf{with\ \phi_2 \geq T_t \geq\ \phi_4} \\ \mathbf{\phi_1^*[(T_t - \phi_2)^{\phi_3}(\phi_4 - T_t)^{\phi_5}]/_I} \quad \mathbf{with\ \phi_2 < T_t <\ \phi_4} \end{cases}$$ Equation 5

The generalized beta function is normalized by $I = \int_{T_t=\phi_2}^{T_t=\phi_4} \phi_1^*[(T_t - \phi_2)^{\phi_3}(\phi_4 - T_t)^{\phi_5}]$.

Temperature parameter values were also obtained from Dalla Pria *et al.* (2006): ϕ_1 = 0.0264, ϕ_2 = 12.725; ϕ_3 = 1.465; ϕ_4 = 40.55, and ϕ_5 = 0.7575.

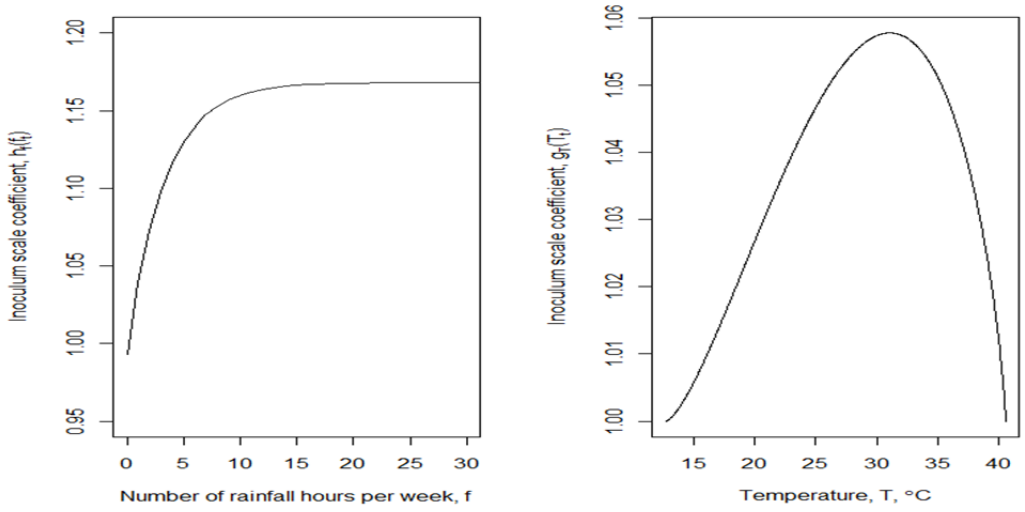

Figure 4. Variation in infectiousness after Dalla Pria *et al.* (2006). Left-hand panel: The effect of the number of rainfall hours on citrus canker infectiousness, represented as a scale coefficient, modelled using a monomolecular relationship: $\boldsymbol{h_f(f_t;b) = b_1[1 - b_2\exp(-b_3 f_t)]}$, where b_1 = 1.168; b_2 = 0.15, and b_3 = 0.305. Right-hand panel: The effect of temperature on citrus canker infectiousness, represented as a scale coefficient. A generalized beta distribution was used, $\boldsymbol{g_T(T_t;\phi) = \phi_1^*[(T_t - \phi_2)^{\phi_3}(\phi_4 - T_t)^{\phi_5}]}$, where ϕ_1 = 0.0264, ϕ_2 = 12.725; ϕ_3 = 1.465; ϕ_4 = 40.55, and ϕ_5 = 0.7575.

4.5. Dispersal Mechanisms

Entry of citrus canker into the network of AOIs, and dispersal between AOIs, can be classified in four categories: illegal importation of bacterial cultures or infected hosts; contaminated introduction of legally traded/moved host or other material, and natural incursions. In the model, the user determines initial entry of citrus canker into the network of AOIs. That is, AOIs can be selected at random and infected at time zero to simulate a natural incursion event, or the user can select specific AOIs that represent likely entry (e.g., illegal importation). Once a node is infected, the disease can spread to other uninfected AOIs via a number of dispersal mechanisms.

4.6. Anthropogenic dispersal mechanisms

The following anthropogenic dispersal mechanisms, i.e., known trace events, were modelled using the half-normal function:

- Introduction of the bacteria in concert with mechanical damage and disturbance of citrus trees due to routine horticultural tree care such as mowing, pruning, hedging harvesting and spraying equipment (Gambley *et al.* 2009, Gottwald and Irey 2007) has been shown to disperse the bacteria within and between neighbouring blocks of citrus (Das 2003).
- Movement of bacteria on clothing, and farm tools e.g., picking bags, clippers.
- Movement of diseased propagating material, budwood, rootstock seedlings or budded trees is the primary cause of long-distance citrus canker dispersal events (Gottwald *et al.* 1989, Das 2003).

The half-normal distribution was used because it is bounded between zero and positive infinity, and since dispersal distances cannot be negative, it was appropriate. The half-normal is also commonly used in distance sampling for detectability (Buckland *et al.* 2001). We allowed the half-normal variance parameter, $\sigma^2{}_d$, to vary for each AOI type.

$$\boldsymbol{f(d;\sigma^2{}_d) = \exp(-d^2/\sigma^2{}_d)} \qquad \text{Equation 6}$$

We simulated contact between two AOIs due to movement of infected farm machinery. Such dispersal and establishment mechanisms were modelled as either inter-AOI distance-dependent functions, e.g., half-normal, or as distance independent Bernoulli trials. Models for transmission probabilities can also be directional between different AOI types. For example, the contact type between a “nursery” AOI and a “backyard” AOI can be different from a “nursery” to an “orchard” AOI. A baseline rate of contact from one AOI type to another is independently specified for movement in each direction between each pair of AOI types (Table 3). Dispersal and establishment function parameters (contact rates) may be altered over time, which is how the model incorporates wind-driven dispersal.

There is no record of seed transmission of citrus canker (Das 2003). Commercial shipments of diseased fruit are potentially a means of long-distance spread, but there is no authenticated record of this happening (Das 2003). Although we do not consider these dispersal mechanisms explicitly for citrus canker, should the model be applied to another pest, the dispersal mechanisms can be changed to accommodate seed dispersal. Fruit can disperse inoculum, but this dispersal mechanism is very unlikely. We implicitly account for the possibility of fruit-based dispersal using the ‘unknown’ dispersal mechanism.

4.7. Weather-based dispersal and establishment mechanisms

We used a half-normal based-function to model the wind speed based component of citrus canker dispersal:

$$\mathbf{f}(\boldsymbol{d};\boldsymbol{\sigma}_{d,t}) = \exp\left\{-\frac{d^2}{2\sigma_{d,t}{}^2}\right\} \qquad \text{Equation 7}$$

where *d* is the inter-AOI distance, calculated from AOI edges. The above formulation yields a probability of establishment and dispersal of *f* = 1 at *d* = 0. Changes in dispersal caused by variation in wind speed, *w*, (units: ms^{-1}) were incorporated into the simulation by modifying the half-normal variance parameter at each time-step, $\sigma^2{}_{d,t} = w_t - k$. The wind speed below which no wind-based dispersal can take place, *k*, was 8 ms^{-1}, after Gottwald and Irey (2007).

The direction-dependence of dispersal by wind, $w(\theta;\ \mu_t, \sigma_t)$ was modelled using a wrapped normal distribution:

$$w(\theta;\ \mu_t, \sigma_t) = \frac{1}{\sigma_t\sqrt{2\pi}} \sum_{k=-\infty}^{\infty} exp\left\{\frac{-(\theta - \mu_t - 2\pi k)^2}{2\sigma_t^2}\right\}$$

where μ_t is the mean wind direction at time step *t* (units: degrees), σ_t is the standard deviation of the wind direction at time step *t* (units: degrees), and θ is the angle between the source (contagious) AOI and a destination AOI. The probability of wind-based (both speed and direction) dispersal is the product of two Bernoulli trials, one conducted on wind-speed based dispersal, $f\left(d; \sigma_{d,t}\right)$, the other wind-direction based dispersal, $w(\theta;\ \mu_t, \sigma_t)$.

Extreme weather events such as hurricanes act as a mechanism of long distance dispersal. Dispersal over distances up to 12 km, can occur during severe tropical storms (Das 2003, Gottwald *et al.* 2001, Gambley 2009). Predicting spread under such circumstances is problematic, because depending on whether the 'front' side of the storm or the 'back' side of the storm crossed over an infected tree, inoculum would spread in opposite directions (Gottwald and Irey 2007, Irey *et al.* 2006). We do not explicitly account for extreme weather events in this model (but see Discussion).

In a standardised experiment (i.e., a fixed amount of inoculum placed on to citrus trees, sprayed with a hose, and exposed to a fan to blow inoculum onto collection plates at certain distances from the citrus trees), Bock *et al.* (2005) concluded that greater than 90% of dispersing bacteria collected 1 m from the source. Wind-dispersed inocula have been observed up to 32 m from a source plant. This suggests the majority of wind/rain dispersal events are likely to contribute to bacterial dispersal a few metres from the source (Bock *et al.* 2005) thus contributing to within-plant and within-AOI dispersal of the bacteria. Wind and rain dispersal are unlikely to contribute to between-AOI dispersal, unless AOIs are very close (e.g., neighbouring citrus blocks within an orchard). Das (2003) also states spread of canker bacteria by wind and rain is mostly over short distances, i.e., within trees or to neighbouring trees.

523
524 **Table 3. Dispersal mechanisms accounted for in this model. Any number of dispersal**
525 **mechanisms can be defined by the user, some of which might be foreseeable for**
526 **citrus canker dispersal, but not explicitly accounted for in our model (e.g., severe**
527 **storms). Plots of example dispersal mechanisms are shown in Appendix 2.**
528

Dispersal mechanism	Distance
Infected farm equipment (e.g., pruners, hedge trimmers)	Short: within tree, and between neighbouring trees (i.e., within AOI). Unlikely to occur between AOIs, unless the AOIs are neighbouring.
People (e.g., contamination on clothing or picking bags)	As per infected farm equipment. Workers could disperse citrus canker to another region e.g., Emerald to Central Burnett within one day.
Wind-driven rain	Short: observed dispersal distances up to 32 m.
Birds	Civerolo (1981) mentions these as a means of dispersal in a review paper, but bird dispersal is considered a rare event and not explicitly accounted for in our model.
Seeds	Unlikely.
Fruit	Long: Viable citrus canker bacteria has been isolated from lesions observed on fresh fruits imported from Uruguay and Argentina into Spain (Golmohammadi *et al.* 2007). Likewise Ibrahim and Al-Saleh (2009) were able to detect viable bacteria on symptomatic fresh citrus fruits in shipments from Pakistan and China to Saudi Arabia. Movement of fruit is not modelled explicitly in this simulation study, but included implicitly using the 'unknown' dispersal mechanism. Further simulation studies could be undertaken in the future that explicitly incorporate fruit movement.
Unknown	Dispersal mechanisms that occur and that are not explicitly modelled.
Propagation material	Long: most likely cause of long distance dispersal is movement of infected budwood, root stock, etc. (Gambley *et al.* 2009).

4.8. Disease detectability within an AOI

Detectability relates to two processes. Initially, the detection of citrus canker present within the region typically has a relatively low probability, since people are not deliberately looking for the disease. Once the disease is detected, detectability will be higher, as awareness is increased and more people are looking for the disease. Detectability can operate at three levels:

(i) the detectability of nodes with susceptible hosts (see Discussion);
(ii) host plant detectability within a node (see Discussion), and
(iii) citrus canker detectability within a host plant.

Node and host plant detectability must be defined by the user when a specific geographic area is simulated (see Discussion).

Citrus canker detectability within a host plant

The probability of detecting citrus canker is a function of whether the symptoms of the disease will be observed and recognised, whether that observation will be reported to relevant authorities and follow-up tests of host material detect the presence of the disease. Whether symptoms of the disease are observed is a function of time: in optimal conditions, lesions are visible after 5 days post-infection, whereas in adverse conditions, lesions might take up to 60 days to become detectable.

We assume there are no false positive disease detections (e.g., in northern Australia water-soaked areas often develop around scab lesions and are easily confused with canker lesions, pers. comm. Pat Barkley, see Discussion). Detectability of the disease changes with level of surveillance (i.e., the greater the proportion of trees surveyed, the greater the chance of detecting the disease, if present), and tree size (Gambley *et al.* 2009).

The detection of citrus canker via visual inspection is conditional on detection of the infected host plant and the presence of citrus canker in the inspected host plant. The post-infection time of a given AOI, $t_{I,i}$, was used to estimate a time-dependent detectability, with a minimum time period, $t_{I,thres}$ of two weeks before visual detection is possible. We model citrus canker detectability as a function of age of infection and infectiousness:

$$\mathbf{d_i}(\mathbf{t}, \mathbf{C_i}; \boldsymbol{\theta}, \mathbf{t}_{I,thres}) = \begin{cases} \mathbf{0 \text{ with } t}_{I,i} < \mathbf{t}_{I,thres} \\ \mathbf{h_i}(\mathbf{C_i}; \boldsymbol{\theta}) \text{ with } \mathbf{t}_{I,i} \geq \mathbf{t}_{I,thres} \end{cases} \quad \text{Equation 8}$$

In this formulation, $h_i(C_i; \boldsymbol{\theta})$ is a logistic function (Figure 5~~Figure 5~~), with the initial probability of detection, $\boldsymbol{\theta}_1$ and shape parameter, $\boldsymbol{\theta}_2$, and depend on within node relative citrus canker infectiousness, C_i, giving:

$$\boldsymbol{h_i}(\boldsymbol{C_i}; \boldsymbol{\theta}) = \frac{\mathbf{1}}{\mathbf{1}+(\mathbf{1}/\boldsymbol{\theta_1})\mathbf{exp}\{-\boldsymbol{\theta_2}\times\mathbf{ln}(\mathbf{C_i})\}} \quad \text{Equation 9}$$

Detectability can be set to change at each time step, if required by the user.

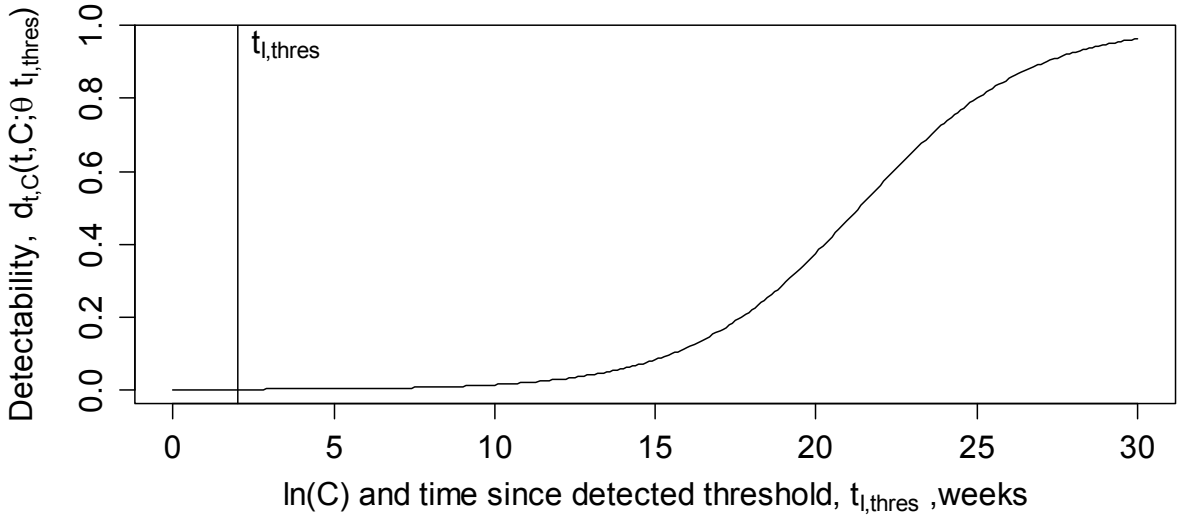

Figure 5. Probability of citrus canker detection in an infected AOI, $\boldsymbol{d_{t,C}(t, C; \theta, t_{I,thres})}$, is dependent upon AOI infectiousness C, and time since infection, *t* (Equation 7). Curve plotted for parameters initial probability of detection $\boldsymbol{\theta_1}$= $3x10^{-4}$, and shape parameter $\boldsymbol{\theta_2}$ = *0.38*; $t_{I,thres}$ = *2*.

4.9. Tracing

Using simulated data we know the details of spread of the pest, so we can test the efficacy of search strategies. For each search strategy there is a trade off between effort (visiting AOI on the network) and detecting infected AOIs. That is, the most effective trace strategy results in the maximum number of infected AOIs found, with the least amount of effort (i.e., without visiting all AOIs on the network). Ideally, the number of AOIs visited is equal to the number of infected AOIs resulting in all infected AOIs being found. We calculated the proportion of AOIs visited by each search strategy, compared to the number of infected AOIs detected, as a metric to investigate the effectiveness of each tracing strategy. We investigated four search strategies:

1. *Adaptive radius*: A circular search area was established around the first detected node (N.B., this is not necessarily the node that was the first infected). The radius of this circle was proportional to the number of months, t_I, since the node was first infected $r = t_I d$, where *d* is an arbitrary distance. This type of search makes no assumptions about search direction (forward or backward tracing). In the citrus canker example, we varied *d* from 50 m to 1,000 m in intervals of 50 m. We used a truncated normal distribution to model the increasing uncertainty in estimating day 0, with increasing time since infection.
2. *Closest n AOIs*: a given number, *n*, of nodes closest to the node where the disease was first detected were searched, with inter-node distance calculated as Euclidian distance from node-edge to node-edge. This type of search makes no assumptions

about search direction. In the citrus canker example, we varied the number of closest *n* nodes from 1 to 100, in steps of 1.

3. *Adaptive search of probability space*: This search strategy is also centred on the node where a disease outbreak is initially detected. Using knowledge of dispersal and establishment probabilities, a matrix of all possible dispersal and establishment probabilities was calculated from each node, to every other node, in the network (Figure 6~~Figure 6~~). This two-dimensional square matrix has dimensions equal to the number of nodes in the network. Each element in the matrix is the probability of disease dispersal *and* establishment from a source node to a destination node. If dispersal and establishment properties were equal between different node types (i.e., non-directional), then the matrix would be symmetrical. In the citrus canker example, we varied the number of nodes searched, *n*, from 1 to 15. The column in the matrix containing the infected node is extracted to form a vector of dispersal and establishment probabilities (one element for each node in the network). The extracted vector was ranked high-to low and the first *n* nodes examined for infection. The search strategy then enters a recursive mode where a vector is extracted, ranked, and examined at each infected node. This recursive model continues until no more infected nodes are detected.
4. *Ranked Pr(disp) search*: where *n* most probable dispersal and establishment pathways are searched (Figure 6~~Figure 6~~). When the first infected AOI was detected, the Pr(disp) space search strategy examined *n* AOIs ranked by Pr(disp), in descending order, in the forward and backward directions from the detected AOI. The technique searches dynamically until no more infected AOIs are found. For example, if an infection was detected at AOI #15, then row 15 (forward searching) and column 15 (backward searching) of the Pr(disp) matrix (Figure 6~~Figure 6~~) are ranked in descending order with *n* unique AOIs being searched. Should infected AOIs be detected during the search, their AOI number would be used to form the starting point of a new search, with the search process continuing until no more infected AOIs are found. For example: *n* =10, so 10 AOIs were searched from the ranked vector Pr(disp) in descending order. The search yielded three infected AOIs from a total of 15 AOIs searched = {45, 46, 43}. The search was continued from each infected AOI to include a further set of 10 ranked AOIs (with already searched AOIs excluded). This search yielded: from AOI #45, zero infected AOIs found; from AOI #46, zero infected AOIs found; and from AOI #43, one infected AOI found (AOI #71). The searched continued from AOI #71, with zero infected AOIs found.

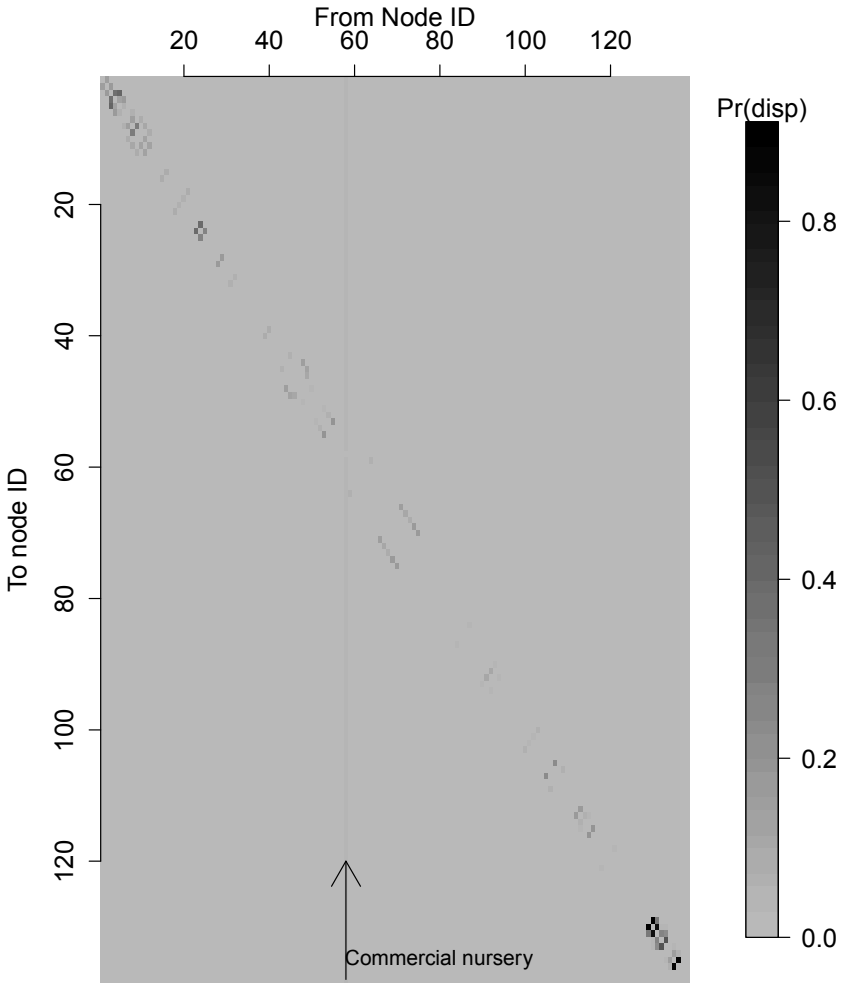

Figure 6. Example of probability of dispersal and establishment space. Matrix elements with a high Pr(disp) are red, low Pr(disp) blue. In this example, the vertical line at AOI number 59 (a commercial nursery) represents different dispersal and establishment mechanisms from the nursery to citrus farm vs. citrus farm to commercial nursery.

All search strategies allow search parameters to be changed. For the “adaptive radius search” the search parameter is search circle radius per month of AOI infection. “Closest *n* AOIs” and “Adaptive search of probability space” search on the number of AOIs, and “ranked Pr(disp)” uses the number of dispersal and establishment pathways.

5. Simulation scenarios

As a result of the wide range of values and combinations of parameters that can be entered, a broad array of specific scenarios can be run for citrus canker dispersal before it is detected at any infected AOI. We ran two simulation scenarios, each based on one geographic region (Emerald, Queensland; Figure 7~~Figure 7~~). In each simulation scenario the initially infected AOI was selected at random. In the first simulation study, we used local weather data from Emerald. In the second simulation study, we used weather data from Mildura (Figure 8~~Figure 8~~). Weather data were taken from between July 2009 to July 2010. Daily temperature and wind gust measurements were converted into a weekly value by using the maximum temperature and wind gust for each week.

Weather influences model output by affecting the infectiousness and susceptibility of an AOI, and by varying wind-based dispersal. Using an example AOI with 1,000 2-yr old citrus trees of the same variety, the influence upon the modelled spread and detectability of citrus canker for two different weather datasets from Emerald (black line; Figure 8~~Figure 8~~) and Mildura (grey line; Figure 8~~Figure 8~~) is shown. Differences in the probability of dispersal and detection are mainly driven by higher temperatures occurring in Mildura (maximum temperature 41.1 ºC) *cf* Emerald (maximum temperature 36.7 ºC).

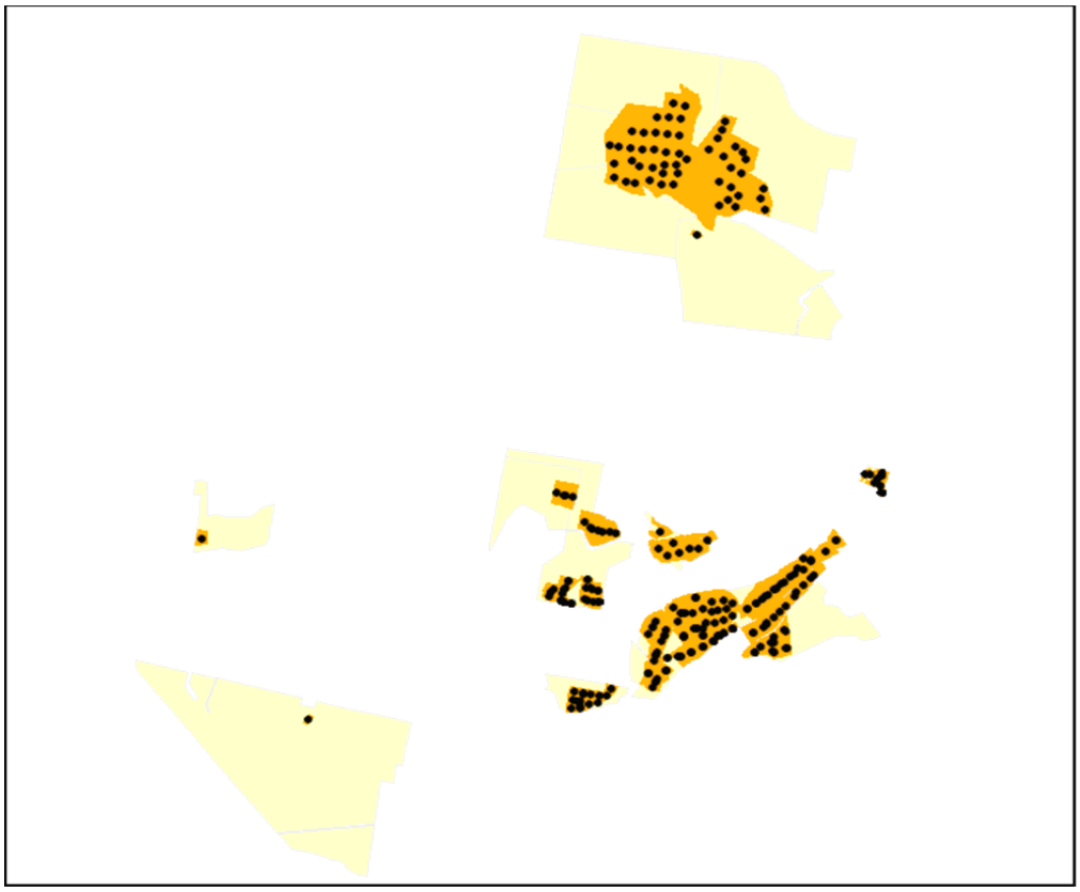

Figure 7. Map of hypothetical citrus-growing region (based on Emerald, Queensland), with areas of citrus trees represented as a network of AOIs. Each AOI (solid black dot) is defined by a spatial location and area, and contains a number of citrus plants, with a mean-tree age. Areas shaded dark orange and yellow are commercial citrus growing areas, and properties that contain commercial citrus areas, respectively.

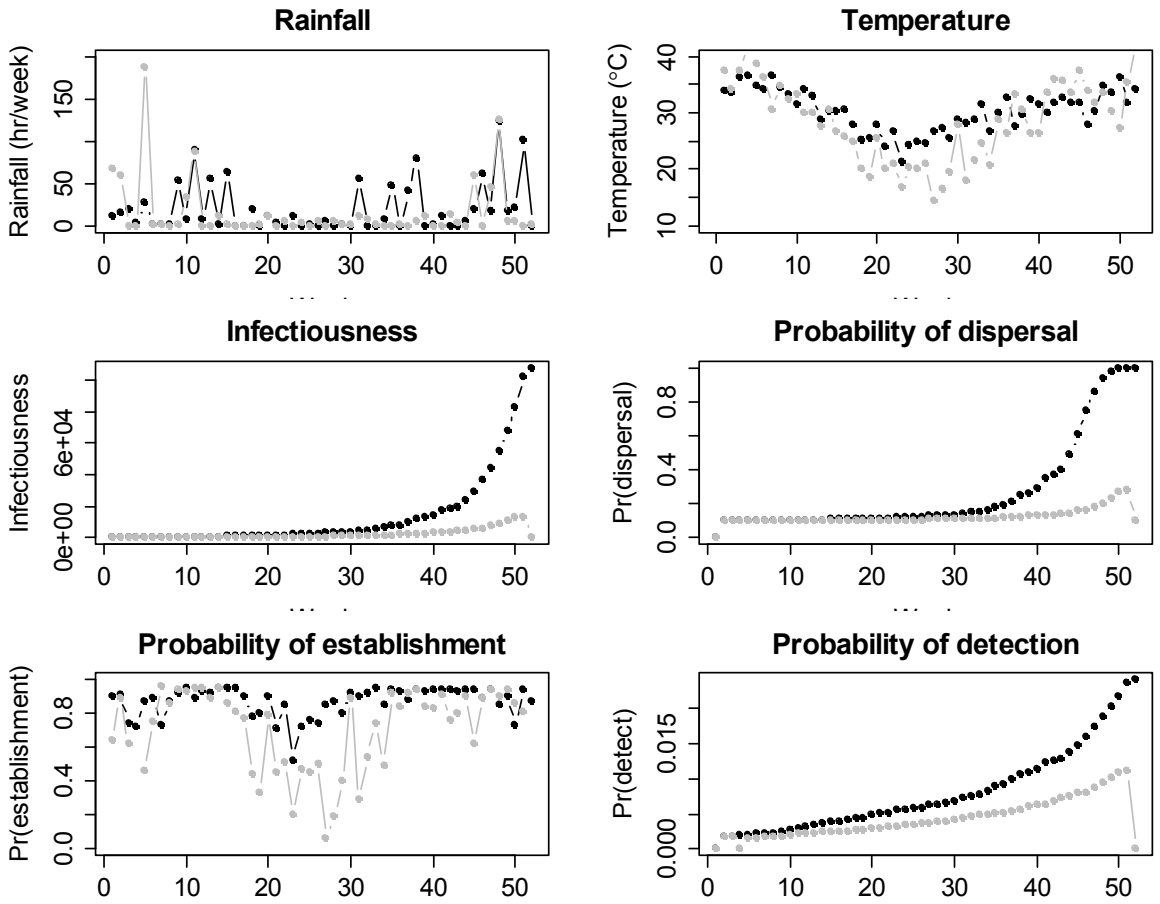

Figure 8. Weekly time series of weather data (x-axis weeks from 1 Jan), and modelled AOI attribute values. First row panels show weekly rainfall duration and temperature from the Australian Bureau of Meteorology for Emerald, QLD (black line) and Mildura, VIC (grey line). Model results are shown in rows two and three: Infectiousness is calculated for an AOI containing 1,000 2-year old trees. Dispersal probability is dependent upon infectiousness, and duration of infection. Establishment probability is based upon citrus variety, mean tree age and temperature. Detection probability is proportional to ln(infectiousness).

6. Results

Each specific model can be run many times to provide distributions of outcomes of interest and descriptive statistics such as the mean, range, standard deviation and selected percentiles for the outcomes (Harvey *et al.* 2007). Since infection is a stochastic process, each realisation of the model will lead to a different epidemic with different AOIs being infected on different days, just as any two real epidemics will be different (Medley 2001).

6.1. Summary Statistics

Each simulation was run for two years, in weekly time steps, making simulation output large. For each simulation, the time step at which a dispersal event occurred is recorded, along with the AOI the citrus canker came from, the AOI(s) it went to, and the dispersal mechanism (e.g., Table 4).

Table 4. Examples of dispersal events from a single run of the simulation model.

Time Step	fromNodeID	fromNodeType	toNodeType	transmissionType
8	59	citrusFarm	citrusFarm	plant
11	131	citrusFarm	citrusFarm	machinery
14	130	citrusFarm	citrusFarm	machinery
16	129	citrusFarm	citrusFarm	plant

In one thousand iterations of each simulation, in some iterations of the simulation, either no spread occurred from the point of initial infection (Emerald: 3.1%; Mildura: 42.7%), or the disease spread but remained undetected during surveillance (Emerald: 0.1%, Mildura: 18.5%).

As time progressed in the simulation, the number of AOIs infected that were detected increased as a non-linear proportion of the total number of AOIs that were infected (Figure ~~Figure~~ 9). The detected proportion was typically greater in Emerald, where weather conditions were more conducive to citrus canker spread, than Mildura where fewer AOIs became infected.

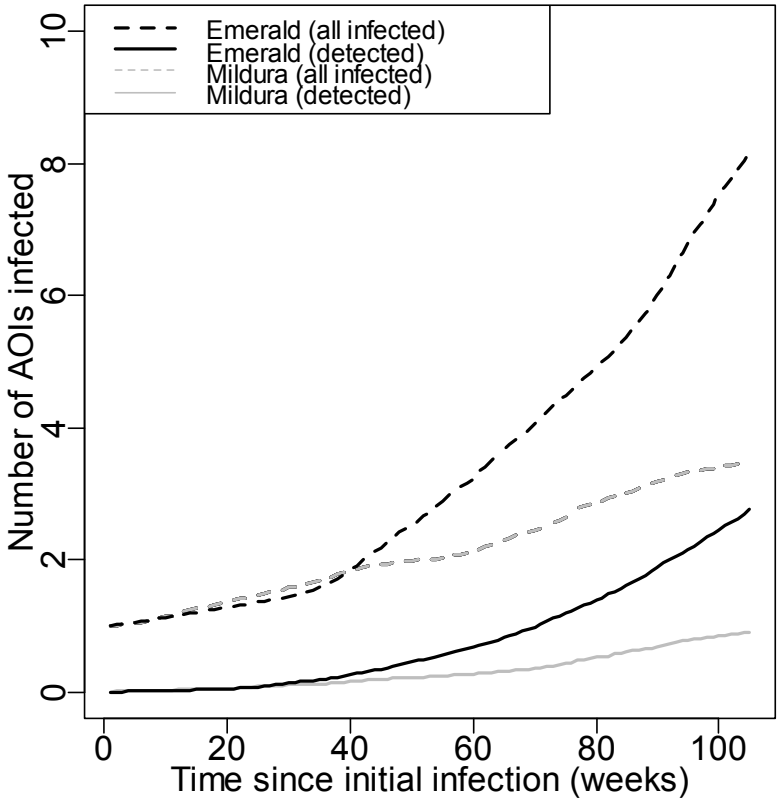

Figure 9. As time progresses in the simulations since time of true day 0 (x- axis), the number of AOIs infected that are detected increases non-linearly with respect to time.

6.1. Tracing outputs

We compared the performance of tracing methods by comparing the proportion of infected AOIs found with the proportion of AOIs searched. We also considered the affect of citrus canker detectability upon tracing performance. To do this, we assumed that after a citrus canker outbreak was detected, management would switch from a 'passive search mode' (Figure 5~~Figure 5~~) to actively searching for citrus canker.

Regardless of which simulation parameters were used and probability of detecting citrus canker if present (set at 1.0, 0.9, 0.7, 0.5 and 0.3), the "adaptive radius" search method always outperformed other search methods (Figure 10~~Figure 10~~-Figure 14~~Figure 14~~). When the weather was cooler (i.e., Mildura) and generally susceptibility of AOIs was less (Figures 10-14B), and detectability was high (Figure 10~~Figure 10~~), the benefit of the top two performing methods was less ("adaptive radius" and "Pr space"). As detectability decreased, the noise in the two worst performing methods ("closest n AOIs" and "ranked Probability") increased. Note, in Figure 10~~Figure 10~~-Figure 14~~Figure 14~~, the y-axis range varies.

When the weather was warmer (i.e., Emerald compared with Mildura) and typically susceptibility of AOIs was higher, the "adaptive radius" method outperformed all other methods tested (Figures 10-14A). However, typically the "closest *n* AOIs" performed better

718 than “Pr space” unless detectability was very low, in which case “Pr space” performed better.
719 Most importantly, no trace technique resulted in 100% of infected AOIs being detected
720 without searching all the AOIs in the map (noting that all AOIs in the network possessed
721 potential host material).

722

(A) (B)

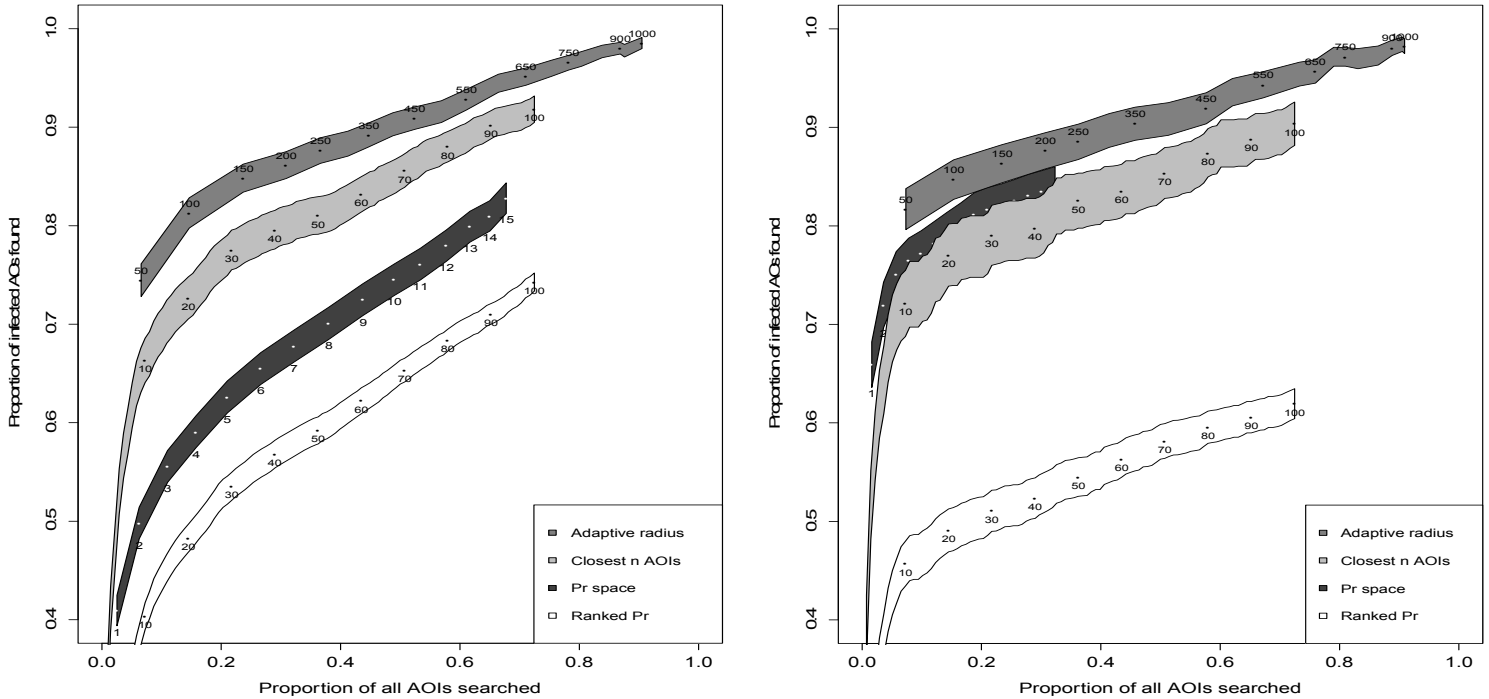

Figure 10. Trace method performance using Emerald region spatial data with dispersal and establishment parameter set based on (A) Emerald and (B) Mildura weather data (c.f. Figure 8~~Figure 8~~). Probability of detecting citrus canker at an infected AOI was 1.0. Trace strategies colour coded, with points showing mean performance annotated by strategy-type search criteria: search radii for adaptive radius; number of nodes searched for closest n nodes, probability space and ranked probability searches. Ribbons are the +/- 2 standard errors calculated from 1,000 simulations (see Section 3).

(A) (B)

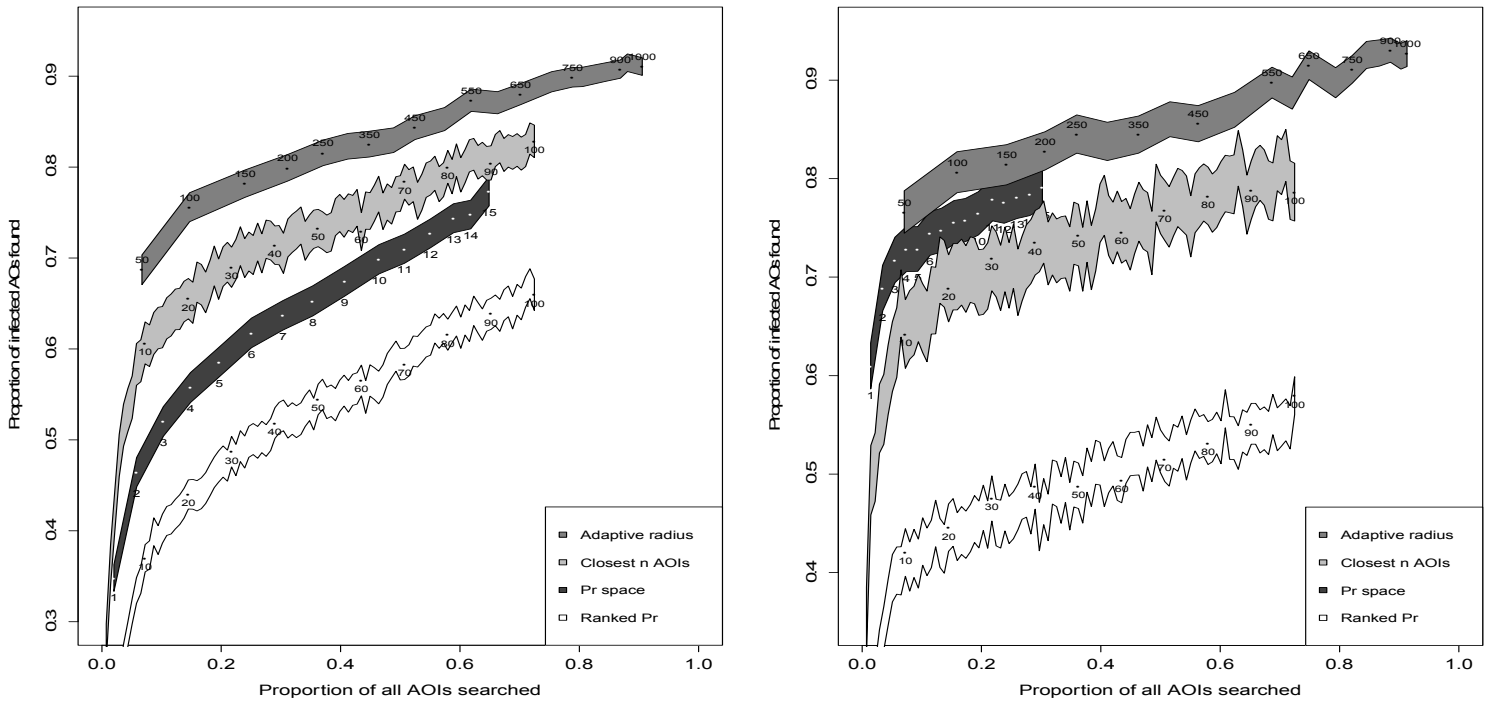

Figure 11. Trace method performance using Emerald region spatial data with dispersal and establishment parameter set based on (A) Emerald and (B) Mildura weather data (c.f. Figure 8~~Figure 8~~). Probability of detecting citrus canker at an infected AOI was 0.9. Trace strategies colour coded, with points showing mean performance annotated by strategy-type search criteria: search radii for adaptive radius; number of nodes searched for closest n nodes, probability space and ranked probability searches. Ribbons are the +/- 2 standard errors calculated from 1,000 simulations (see Section 3).

(A) (B)

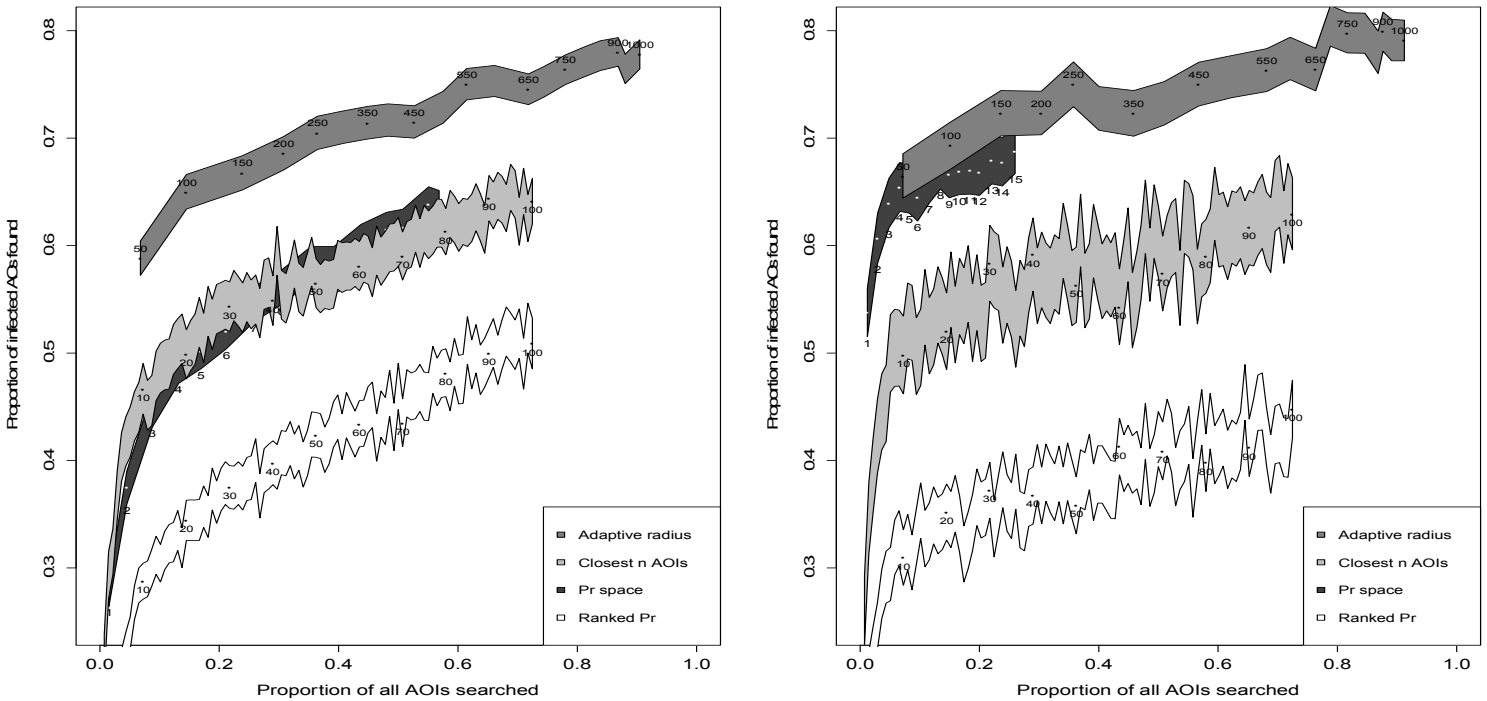

Figure 12. Trace method performance using Emerald region spatial data with dispersal and establishment parameter set based on (A) Emerald and (B) Mildura weather data (c.f. Figure 8~~Figure 8~~). Probability of detecting citrus canker at an infected AOI was 0.7. Trace strategies colour coded, with points showing mean performance annotated by strategy-type search criteria: search radii for adaptive radius; number of nodes searched for closest n nodes, probability space and ranked probability searches. Ribbons are the +/- 2 standard errors calculated from 1,000 simulations (see Section 3).

(A) (B)

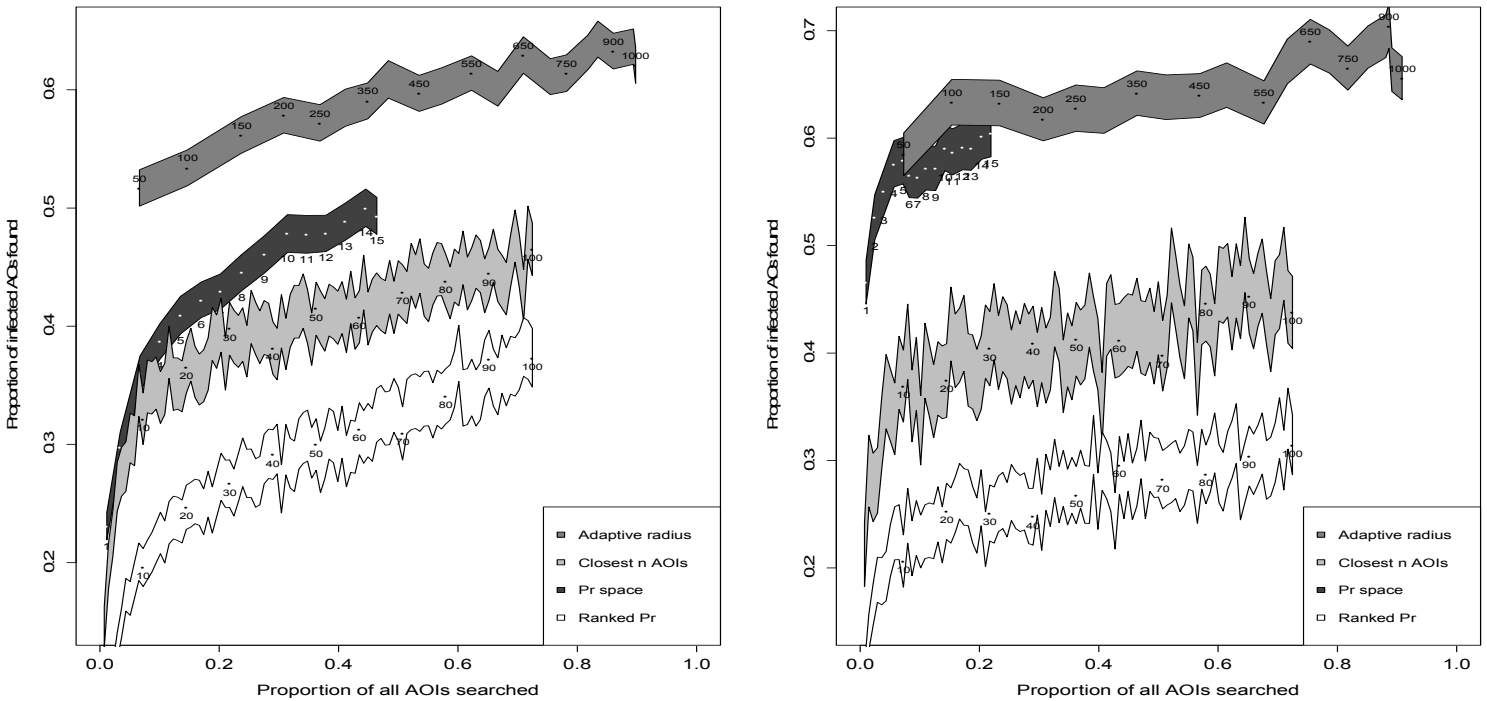

Figure 13. Trace method performance using Emerald region spatial data with dispersal and establishment parameter set based on (A) Emerald and (B) Mildura weather data (c.f. Figure 8~~Figure 8~~). Probability of detecting citrus canker at an infected AOI was 0.5. Trace strategies colour coded, with points showing mean performance annotated by strategy-type search criteria: search radii for adaptive radius; number of nodes searched for closest n nodes, probability space and ranked probability searches. Ribbons are the +/- 2 standard errors calculated from 1,000 simulations (see Section 3).

(A) (B)

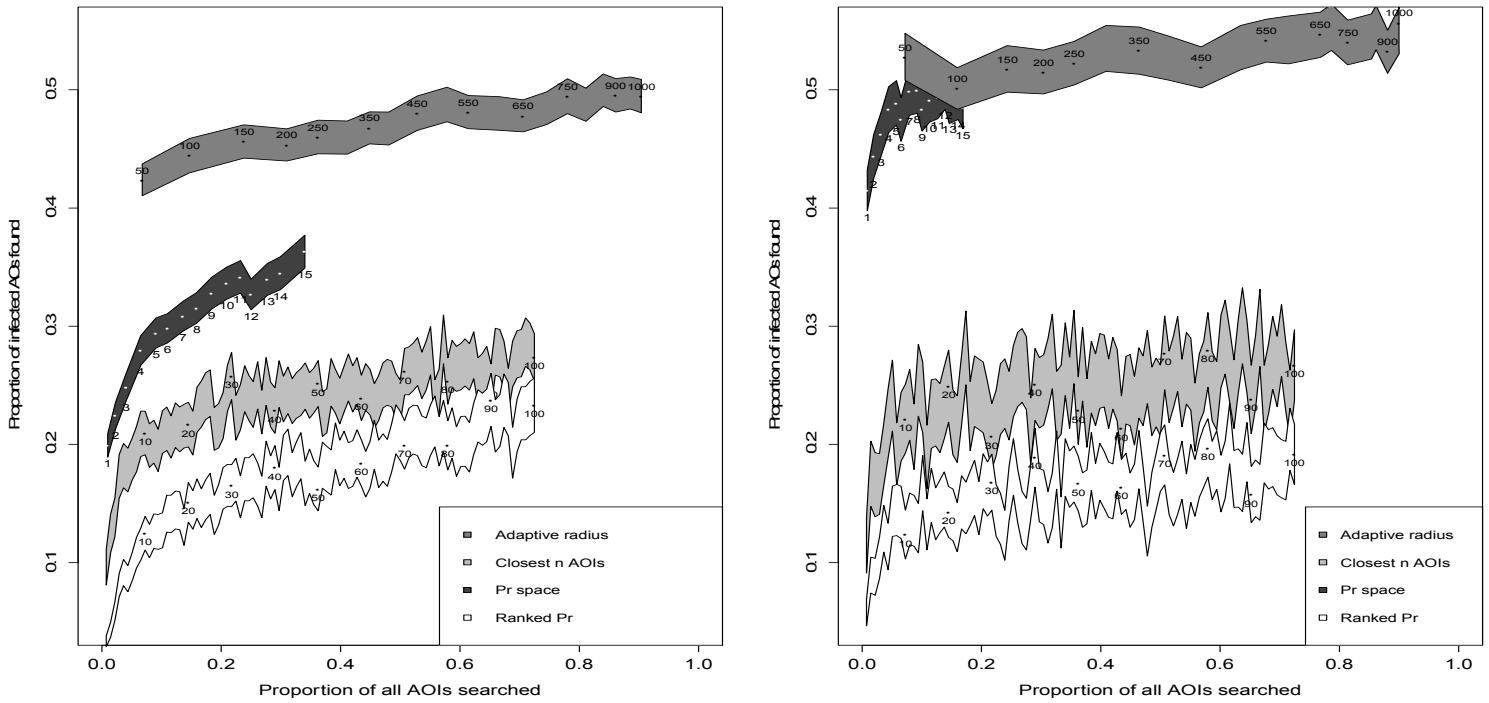

Figure 14. Trace method performance using Emerald region spatial data with dispersal and establishment parameter set based on (A) Emerald and (B) Mildura weather data (c.f. Figure 8~~Figure 8~~). Probability of detecting citrus canker at an infected AOI was 0.3. Trace strategies colour coded, with points showing mean performance annotated by strategy-type search criteria: search radii for adaptive radius; number of nodes searched for closest n nodes, probability space and ranked probability searches. Ribbons are the +/- 2 standard errors calculated from 1,000 simulations (see Section 3).

7. Discussion

7.1. Key findings

- Regardless of model input parameters (e.g., weather), or imperfect “active detection” – detections that occur after the initial detection of an infected AOI– the “adaptive radius” trace priority strategy always outperformed the other three strategies we tested.
- None of the trace priority strategies consistently found all infected AOIs without searching all susceptible AOIs in a geographical area.
- The model is sensitive to area-specific weather.

It is imperative that all susceptible AOIs are known and the spatial location of all hosts can be mapped for the disease of interest. If areas of interest contain susceptible hosts, and these are unknown (or hidden), then eradication may be impossible if these susceptible AOIs act as a continual source of reinfection.

7.2. Implementation of model outputs for BioSIRT

The need for an efficient, consistent and nationally-coordinated approach to manage information during routine biosecurity surveillance activities and emergency responses to incursions of animal or plant diseases in Australia led to the development of the web-based software application BioSIRT (Biosecurity Surveillance Incident Response and Tracing, see: http://www.daff.gov.au/animal-plant-health/emergency/biosirt). Users of BioSIRT include Commonwealth, state and territory agencies that are responsible for management of animal and plant diseases that may threaten the environment and economic activities. BioSIRT links textual information (about routine and emergency incidents) to spatial information about an area of interest (details about land and parties associated with the land). National BioSIRT templates for emergency responses to emergency animal diseases make use of predefined trace priorities for combinations of input variables, developed by technical reference groups for AusVetPlan composed of domain experts (e.g., epidemiologists), and these are implemented. Input variables are specifying the direction of a trace (i.e., forward or backward trace events), the category of the items that have moved between AOIs (e.g., meat, milk, person, vehicle, etc.); number of movement events; the contact type (i.e., direct, indirect) and the date of movement relative to day zero. The combination of input variables is then matched with a pre-defined ‘look-up’ table that automatically assigns that particular combination of events a priority. Technical reference groups composed of domain experts (e.g., epidemiologists) have developed the priorities within the look-up table.

Our model results might improve the trace prioritisation component of BioSIRT for use in plant health emergencies.

7.3. Model performance and ideas for future research

Disease dispersal is a very complex process so representing this complex process in a simplified model will always have limitations. This model was built for exploratory purposes. Due to the large numbers of parameters involved in model, many different simulation scenarios could have been undertaken. Here, we undertook a limited simulation study using weather data from two regions and the same dispersal mechanisms. It would be useful to undertake a larger simulation study to thoroughly investigate different dispersal mechanisms (see Appendix 10).

The simulation model and tracing rule sets have been implemented in the statistical language R. Running on a desktop PC, a simulation spanning two years, with a geographical area containing 138 known nodes and 45 possible dispersal pathways (9 of which were time-dependent) takes four hours to complete 100 realisations.

The model we present in this research was developed with flexibility in mind, thus allowing one to:

1. Investigate the behaviour of different strategies for searching/ prioritising tracing of citrus canker in other regions, by altering the model structure and/or input parameters to those presented here, and
2. Alter model parameters and structure and use this model for other plant pests and diseases.

Here we provide some discussion on future research that can be undertaken by modifying the current model:

7.4. Control measures

Since our aim was to focus on emergency response in the first week or two after detection of citrus canker, we did not implement any control measures. The model does have the flexibility to investigate the affect of control strategies upon disease spread. Currently the model can accommodate two control strategies:

1. Destroy all host material at AOIs at which citrus canker is detected (Das 2003). This might be a useful characteristic of the model, should, for example, someone wish to investigate what might happen during an outbreak in the medium-term (i.e., after citrus canker is detected and assumed eradicable, eradication is not instantaneous but may take a matter of months). The only control measure in our model is that nodes detected with the citrus canker are destroyed (Das 2003). This management action is consistent

with that taken during the 2004 outbreak of citrus canker in Emerald. The model assumes destruction happens within a time step. Keeling (2003) proposes the removal of "key" AOIs (i.e., AOIs that are highly connected to other AOIs) within a network to increase chance of removal, and this could be considered in future research.

2. Post-detection of citrus canker, typically movements of suspect host-material will be stopped by management actions. This can be accommodated in the model by setting time-specific dispersal mechanisms (i.e., prior to detection, dispersal mechanism are as described in Table 2, and post-detection, all anthropogenic dispersal mechanisms – apart from, e.g. wind – can be set to zero), and is important to explore in future research.

7.5. Cost

The model we present does not explicitly include cost. Both the cost of surveillance (pre- and post-infection) and control measures could be estimated. Should control measures (c.f. Section 6.1) be implemented in future research using this model, it is possible to calculate how many AOIs and their characteristics (i.e., number of individual citrus trees within each AOI) are destroyed. This would form a surrogate measure of cost, but would underestimate true cost since e.g., the time taken to destroy each AOI by field personnel is not taken in to consideration. Also, tracing is not instantaneous as searching AOIs takes time. This aspect also requires considerable resources and its costs should not be overlooked.

In addition, the time taken to detect all infected AOIs (note, not one search strategy we investigated detected all infected AOIs on the network without searching all AOIs) could be monitored. Since the aim of most disease outbreaks is to eradicate the disease as quickly as possible, monitoring time taken to detect all infected AOIs is important for decision making and warrants further investigation.

7.6. The spatial distribution of individual plants within an AOI

Our model assumes that the spatial distribution of infected individuals with an AOI does not influence the dynamics and spread of the pest. We know this is not the case, as typically citrus plants that are infected with citrus canker are neighbours within each citrus block. However, in order to run a network-based model, this must be assumed (e.g., Keeling 2005). Other model types can be investigated (e.g., agent-based models) that could account for the location of individual host plants in a landscape.

7.7. Wind dispersal model and other dispersal mechanisms

We used a simple model to account for wind-based dispersal and establishment mechanisms. This model included the direction of prevailing wind and distance between two AOIs. Landscape patterns (e.g., digital terrain data) could be used to modify the wind

dispersal model and eradication effort (Parnell *et al.* 2010), but was not feasible to implement here given the time frame available.

Other dispersal mechanisms and shapes could be defined by the user. The number of distributional shapes is large, and include, e.g. heavy-tailed distributions that have large skewness.

7.8. Severe storms

Severe storms can disperse citrus canker inoculum, with records of distances up to 10 kilometres (Gambley *et al.* 2009). Since we are focusing on emergency response, where the aim is to determine the extent of the citrus canker outbreak and ensure the largest proportion of traces are successful in detecting citrus canker within AOIs, we did not explicitly model severe storms. The model is capable of simulating multiple initially infected AOIs and wind-based injuries to trees, which may increase susceptibility to citrus canker. This could be modeled on an AOI-by-AOI basis.

7.9. Influence of leafminer and mechanical wounds

Leafminers expose the leaf mesophyll, increasing the probability of a direct contact of the citrus canker pathogen with the interior of the host citrus plant (Jesus *et al.* 2006, Hall *et al.* 2010). And according to Goto (1992), wounds caused by mechanical damage heal more quickly, within a few days, whereas wounds caused by the leafminer heal more slowly, making leaf tissues susceptible to infection for longer periods. We did not explicitly account for damage to leaves caused by leaf miner or mechanical injury, which increases susceptibility to citrus canker infection. However, susceptibility could be included implicitly—as for damage caused by severe storms—by changing the susceptibility of each AOI to be higher in the presence of either leaf miner or mechanical damage.

7.10. AOI and host organism detectability

Although not used in the examples presented here, the model has flexibility to include AOI detectability and the detectability of host organisms within an AOI. That is, susceptible AOIs that are undetected, or unknown to management, are called hidden AOIs. Hidden AOIs arise because of imperfect knowledge regarding the spatial location of AOIs and whether host species might be present the hidden AOIs. If infected, hidden AOIs remain on the network, they may act as a source for future re-infection and render the eradication process futile. When an AOI is hidden, unless it is discovered via surveillance or tracing, the AOI will be unavailable to management decision making or monitoring. In the simulator (“real-world”) view, however, the hidden AOI can, if it contains infected host plants trees, disperse citrus canker to other uninfected AOIs.

Undetected host plants within AOIs can also be accommodated in the simulator. Again this is caused by imperfect knowledge and adds another tier of surveillance effort to be expended in order to identify AOIs that contain susceptible or infectious plants.

Although not currently implemented, the effect of false-positive citrus canker detections upon the efficacy of the tracing rule sets could be established.

7.11. Future case studies?

To further develop and test the model, it could be parameterised using other pest or pathogens as case studies. Two potential case studies are Huanlongbing (the cause of citrus greening, http://www.daff.gov.au/aqis/quarantine/naqs/naqs-fact-sheets/citrus-greening) and myrtle rust (*Uredo rangleii*). There is also a National BioSIRT Standards Committee working group finalising an emergency response template for citrus greening, which is disease that affects citrus species. Since it is vector-dispersed, there would be an additional level level of complexity compared to the case study used on citrus canker. Myrtle rust is also a potential case study for which there is a national emergency response template that is a revision of one used in an emergency response in New South Wales in 2010.

7.12. Recommendations

For outbreaks of citrus canker, using the ‘adaptive radius’ trace strategy was the most effective trace strategy of those tested. It would seem reasonable to use this strategy in future outbreaks of citrus canker, but the strategy should not be taken as a ‘hard and fast’ rule, so to speak, and outbreak-specific information and data should be collected and considered on a case-by-case basis. For example, the ‘adaptive radius’ strategy might not work in situations where very long dispersal distances occur, i.e. those from outside the modelled geographical area, and this should be investigated.

The model presented here is reasonably complicated and has extensive code available in the statistical software language R (freely available from www.r-project.org). It should be a priority to formalise the current code into an R package. For developing general rules for trace prioritisation for other pests and diseases of plants, we recommend, the model be parameterised by experts for other such pests and diseases and the results re-analysed, to determine if this tracing search strategy is best.

The questions arise, how far could the model developed here be extrapolated to other pests and diseases; and will the search radius strategy be a generally effective method for setting plant pest emergency response priorities? This is the first model for plant pest emergency response in Australia, and as such, any extrapolation should be considered very carefully. Experience from models for animals suggests that emergency response priorities are likely to

be disease- and context-specific. The caveats outlined below form the first test for any attempt to generalize.

7.13. Caveats

1. The model is currently parameterised and tested for short-range dispersal and establishment within one geographic area. The model has not been used to simulate long-range dispersal, so no inferences can currently be made about citrus canker spreading “off-map” into or from AOIs in other geographic areas.
2. The model should be used to assist in planning surveillance in an emergency response. It is not our intention that the model should overrule surveillance officers’ actions in the field. Rather, we hope the model will be used as a tool to formalise surveillance decisions: when overruling the model we hope people will think critically and justify their actions.
3. Before being applied to other plant diseases, the model must be re-parameterized with disease-specific values and mechanisms. We cannot offer general rules for the surveillance of plant diseases, without further testing and model development. Development of R-code for this model will greatly facilitate the extension of this work to other contexts and species, and eventually, to the development of general prescriptions and rules of thumb for emergency trace priorities for plant pests.

8. References

Alam, K. and Rolfe, J. (2006). Economics of Plant Disease Outbreaks. *Agenda*, 13(2): 133-146.

Bock, C. H., Parker, P. E. and Gottwald, T. R. (2005). Effect of Simulated Wind-Driven Rain on Duration and Distance of Dispersal of *Xanthomonas axonopodis* pv. citri from Canker-Infected Citrus Trees. *Plant Disease*, 89(1): 71-81.

Cacho, O., Spring, D., Hester, S. and Mac Nally, R. (2010). Allocating surveillance effort in the management of invasive species: A spatially-explicit model. *Environmental Modelling & Software*, 25: 444-454.

Dalla Pria, M., Christiano, R. C. S., Furtado, E. L., Amorim, L. and Bergamin Filho, A. (2006). Effect of temperature and leaf wetness duration on infection of sweet oranges by Asiatic citrus canker. *Plant Pathology*, 55(5): 657-663.

Das, A. K. (2003). Citrus canker – A review. *Journal of Applied Horticulture*, 5(1): 52-60.

Fox, J. C., Buckley, Y. M., Panetta, F. D., Bourgoin, J., and Pullar, D. (2009). Surveillance protocols for management of invasive plants: modelling Chilean needle grass (*Nassella neesiana*) in Australia. *Diversity and Distributions.* 15: 577-589.

Gambley, C. F., Miles, A. K., Ramsden, M., Doogan, V., Thomas, J. E., Parmenter, K. and Whittle, P. J. L. (2009). The distribution and spread of citrus canker in Emerald, Australia. *Australasian Plant Pathology*, 38(6): 547-557.

Garner, M. G. and Beckett, S. D. (2005). Modelling the spread of foot-and-mouth disease in Australia. *Australian Veterinary Journal*, 83(12): 758-766.

Garner, M. G. and Hamilton, S. A. (2011). Principles of epidemiological modelling. *OIE Scientific and Technical Review*, 30(2): 407-416.

Garner, M. G., Cowled, B., East, I. J., Moloney, B. J. and Yung, N. Y. (2011). Evaluating the effectiveness of early vaccination in the control and eradication of equine influenza—A modelling approach. *Preventive Veterinary Medicine*, 99: 15-27.

Golmohammadi, M., Cubero, J., Peñalver, J., Quesada, J. M., López, M. M. and Llop, P. (2007). Diagnosis of *Xanthomonas axonopodis* pv. *citri*, causal agent of citrus canker, in commercial fruits by isolation and PCR-based methods. *Journal of Applied Microbiology*, 103(6): 2309-2315.

Goto, M. (1992). Citrus canker. In: *Plant Diseases of International Importance* (Kumar, J., Chaube, H.S., Singh, U.S. and Mukhopadhyay, A.N., eds), pp. 250–269. Englewood Cliffs,

NJ: Prentice Hall.

Gottwald, T. R., Timmer, L. W. and McGuire, R. G. (1989). Analysis of Disease Progress of Citrus Canker in Nurseries in Argentina. *Phytopathology*, 79: 1276-1283.

Gottwald, T. R. and Graham, J. H. (1992). A device for precise and nondisruptive stomatal inoculation of leaf tissue with bacterial pathogens. *Phytopathology*, 82, 930–935.

Gottwald, T. R., Graham, J. H. and Schubert, T. S. (2002). Citrus canker: The pathogen and its impact. *Plant Health Progress*.

Gottwald, T. R. and Irey, M. (2007). Post-hurricane Analysis of Citrus Canker II: Predictive Model Estimation of Disease Spread and Area Potentially Impacted by Various Eradication Protocols Following Catastrophic Weather Events. *Plant Health Progress*.

Gottwald, T. R., Bassanezi, R. B., Amorim, L., and Bergamin-Filho, A. (2007). Spatial pattern analysis of citrus canker-infected plantings in São Paulo, Brazil, and augmentation of infection elicited by the Asian leafminer. *Phytopathology*, 97(6): 674-683.

Graham, J. H., Gottwald, T. R., Riley, T. D., Cubero, J. and Drouillard, D. L. (2000). Survival of *Xanthomonas campestris* pv. *citri* (Xcc) on various surfaces and chemical control of Asiatic citrus canker (ACC). *Proc. Intn. Citrus canker Res.Workshop*. June 20-22, 2000, Ft. Pierce, Florida, p.7.

Graham, J. H., Gottwald, T. R., Cubero, J., and Achor, D. (2004). *Xanthomonas axonopodus* pv. *citri*: Factors affecting successful eradication of citrus canker. *Molecular Plant Pathology,* 5(1): 1-15.

Hagerman, A. D., Looney, J. C., McCarl, B. A., Anderson, D. P. and Ward, M. (2010). Rapid Effective Trace-Back Capability Value in Reducing the Cost of a Foot and Mouth Disease Event, Orlando.

Hall, D. G., Gottwald, T. R. and Bock, C. H. (2010). Exacerbation of Citrus Canker by Citrus Leafminer *Phyllocnistis citrella* in Florida. *Florida Entomologist,* 93:558-566.

Harvey N., Reeves A. P., Schoenbaum M. A., Zagmutt-Vergara F. J., Dubé C., Hill A. E., Corso B. A., McNab B., Cartwright C. I. and Salman M. D. (2007). The North American Animal Disease Spread Model: a simulation model to assist decision making in evaluating animal disease incursions. *Preventative veterinary Medicine*, 82: 176-197.

Ibrahim, M. A., and Al-Saleh, Y. E. (2009). Population dynamics of *Xanthomonas citri* subsp. *Citri* on symptomless citrus fruits under Saudi Arabia conditions and effect of post-harvest treatments on survey of the bacteria. *Journal of Plant Pathology*, (2010), 92 (3): 601-605.

Irey, M., Gottwald, T. R., Graham, J. H., Riley, T. D. and Carlton, G. (2006). Post-hurricane Analysis of Citrus Canker Spread and Progress towards the Development of a Predictive Model to Estimate Disease Spread Due to Catastrophic Weather Events. *Plant Health Progress*, 1-15.

Jeger, M. J., Pautasso, M., Holdenrieder, O., and Shaw, M. W. (2007). Modelling disease spread and control in networks: implications for plant sciences. *New Phytologist*, 174: 279-297.

Jesus, JR., W. C., Belasque, JR., J., Amorim, L., Christiano, R. S. C., Parra, J. R. P., and Bergamin Filho, A. (2006). Injuries caused by citrus leafminer (*Phyllocnistis citrella*) exacerbate citrus canker (*Xanthomonas axonopodis* pv. *citri*) infections. *Fitopatl. Bras.,* 31: 277-283.

Keeling, M. J. (2005). Models of foot-and-mouth disease. *Proceedings of the Royal Society B: Biological Sciences*, 272(1569): 1195-1202.

Koizumi, M. (1974). Studies on the symptoms of citrus canker formed on Satsuma mandarin fruit and existence of causal bacteria in the affected tissues. *Bull. Hort. Res. Sta., Japan, Ser. B,* 12: 229-244.

Koizumi, M. (1981). Resistance of citrus plants to bacterial canker disease: a review. *Proceedings of the International Society of Citriculture,* 1: 402-405

Mangano, P., Hardie, D., Speijers, J. Johnston, R., de Sousa-Majer, M. J., and Maynard, G. (2011). The Capacity of Groups within the Community to Carry out Plant Pest Surveillance Detection. *The Open Entomology Journal*, 5: 15-23.

Parnell S., Gottwald, T. R., Gilligan, C. A., Cunniffe, N. J., and van den Bosch, F. (2010). *Phytopathology*, 100(7): 638-44.

Perry, B., McDermott, J., and Randolph, T. (2001). Can epidemiology and economics make a meaningful contribution to national animal-disease control? *Preventive Veterinary Medicine*, 48(4): 231-260.

Queensland Government Department of Primary Industries and Fisheries (2006). "Emergency Plant Pest Response Plan – Eradication of citrus canker in Queensland (confidential)". Version 4. Dated 19th December 2006.

Reeves, A., Salman, M. D., and Hill, A. E. (2011). Approaches for evaluating veterinary epidemiological models: verification, validation and limitations. *OIE Scientific and Technical Review*, 30(2): 499-512.

Slovic, P. (1999). Trust, emotion, sex, politics, and science: surveying the risk-assessment

battlefield. *Risk Analysis* 19: 689-701.

Spiegel-Roy, P., and Goldschmidt, E. E., (1996). *Biology of Citrus*. Cambridge University Press, Cambridge, 230 pp.

Stall, R. E., Miller, J. W., Marco, C. M. and DeEchenique, B. I. C. (1980). Population dynamics of *Xanthomonas citri* causing cancrosis of citrus in Argentina. *Proceedings of the Florida Horticultural Society* 93: 10-14.

Telford, G. (2005). "Surveillance for establishment of Pest Free Area status for citrus canker – Gayndah and Mundubbera Management Zone (confidential)". Report number ST-R-003, prepared for the Queensland Government Department of Primary Industries and Fisheries. Dated 10th February 2005.

Telford, G. and Higgins, J. (2005). "Overview of tracings investigations for citrus canker on Infested Premises number 1 (confidential)". Report number ST-R-005, prepared for the Queensland Government Department of Primary Industries and Fisheries. Dated 14th June 2005.

Telford, G., O'Brien, M. and Ashton, M. (2009). "Proposal for the establishment of pest free area status for citrus canker – Emerald Pest Quarantine Area for citrus canker (confidential)". Dated 12th January 2009. Prepared for the Queensland Government Department of Primary Industries and Fisheries

Turrell, F.M. (1961). Growth and photosynthesis area of citrus. *Botanical Gazette*, 122: 284-298.

Wilkinson, K., Grant, W. P., Green, L. E., Hunter, S., Jeger, M. J., Lowe, P., Medley, G. F., Mills, P., Phillipson, J., Poppy, G. M., and Waage, J. (2011). Infectious diseases of animals and plants: an interdisciplinary approach. *Philosophical Transactions of the Royal Society B: Biological Sciences*, 366(1573): 1933-1942.

9. Appendix 1: Tree growth models

We have parameterised three candidate tree canopy surface area vs. age relationships:

(i) after Turrell (1961), we used a cubic-spline, or

(ii) linear growth to a fixed age, and constant thereafter, and

(iii) a Richards age-growth curve parameterized using data from juicing orange varieties near Mildura provided by Graeme Sanderson (NSW, Department of Primary Industries).

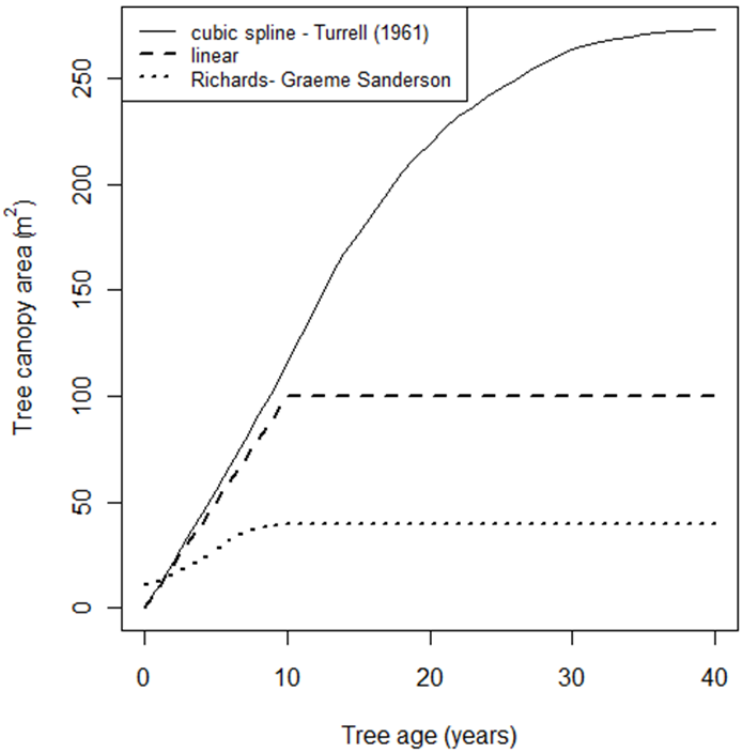

Fig. A1: Parameterised tree citrus tree canopy area ~ age relationships: (i) Turrell (1961) citrus tree surface-area modelled using a cubic-spline (solid line); (ii) linear to 10 years old (dashed line), and (iii) Richards curve parameterized using data from juicing orange varieties near Mildura provided by Graeme Sanderson (NSW, Department of Primary Industries).

9.1. Model implementation information: tree area

Tree canopy area is calculated using the R function `treeAgeAreaFunc(age,curveType, parVec)`.

The Turrell (1961) cubic function (`curveType = "CSPLINE"`) was fitted using `smooth.spline` and saved as an R object `growthAtAgeCSpline.RObj`, which is loaded

into the `parVecInoculum` object using:
`parVecInoculum=dget(paste(globalDir,"growthAtAgeCSpline.RObj",sep="" ))` and then passed into the `treeAgeAreaFunc()`.

The linear relationship (`curveType = "LINEAR"`) is used in the simulation and has parameter vector parVec=c(10,100) which are tree age and which growth stops and maximum tree canopy area.

Parameters for a Richard's curve (`curveType = "RICHARDS"`) were estimated using data provided by Graeme Sanderson was fitted giving `parVec=c(39.5093 , 4.7631, -0.8322 , 6.2830)`.

Growth curve types `curveType = c("RICHARDS","LOGISTIC")` are also available, but have not been parameterized.

10. Appendix 2: Example dispersion and establishment functions

10.1. Model implementation information: dispersal & establishment

Dispersal and establishment parameters (Figure A2) are passed into the model via the `transmissionData` argument in the function `simIterationFunc`. This implementation allows the parameters in `transmissionData` to be changed in each time step, and is currently carried out for wind-based dispersal, but could be extended to any of the dispersal and establishment functions. Dispersal success or failure is determined using a set of nested functions (Fig. A3). Within the `probDrawFunc` Bernoulli trials are conducted on all dispersal and establishment pathways apart from wind-based, which is handled by the function `windDispersalFunc`.

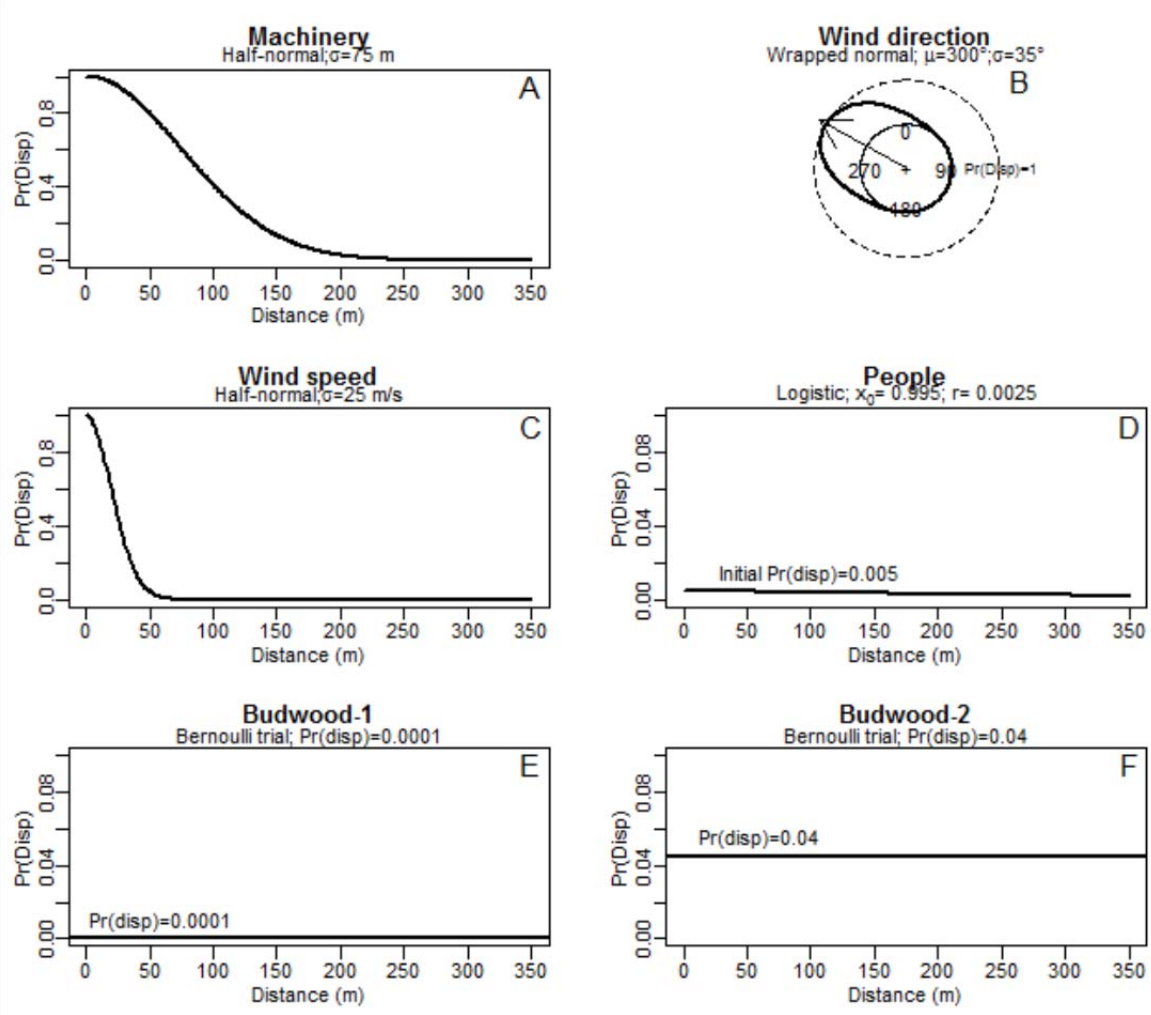

Fig. A2: Example dispersal and establishment weekly probabilities, Pr(disp), for five different dispersal and establishment pathways. Function parameters are given under these panel titles. Wind direction and wind speed based Pr(disp) are varied at each model time-step

based on weather data (see **Error! Reference source not found.**~~Figure 9~~). The budwood pathway, panels E and F have AOI-type dependent parameters with Budwood-1 parameterised with Pr(disp)=0.0001 for citrus block to citrus block and citrus block to commercial nursery. Whereas Budwood-2 was parameterised Pr(disp)=0.04 for commercial nursery to other AOI types. NB varying y-axis scales: panels A and C have Pr(disp) range 0 to1, panels D to F have Pr(disp) range 0 to 0.1.

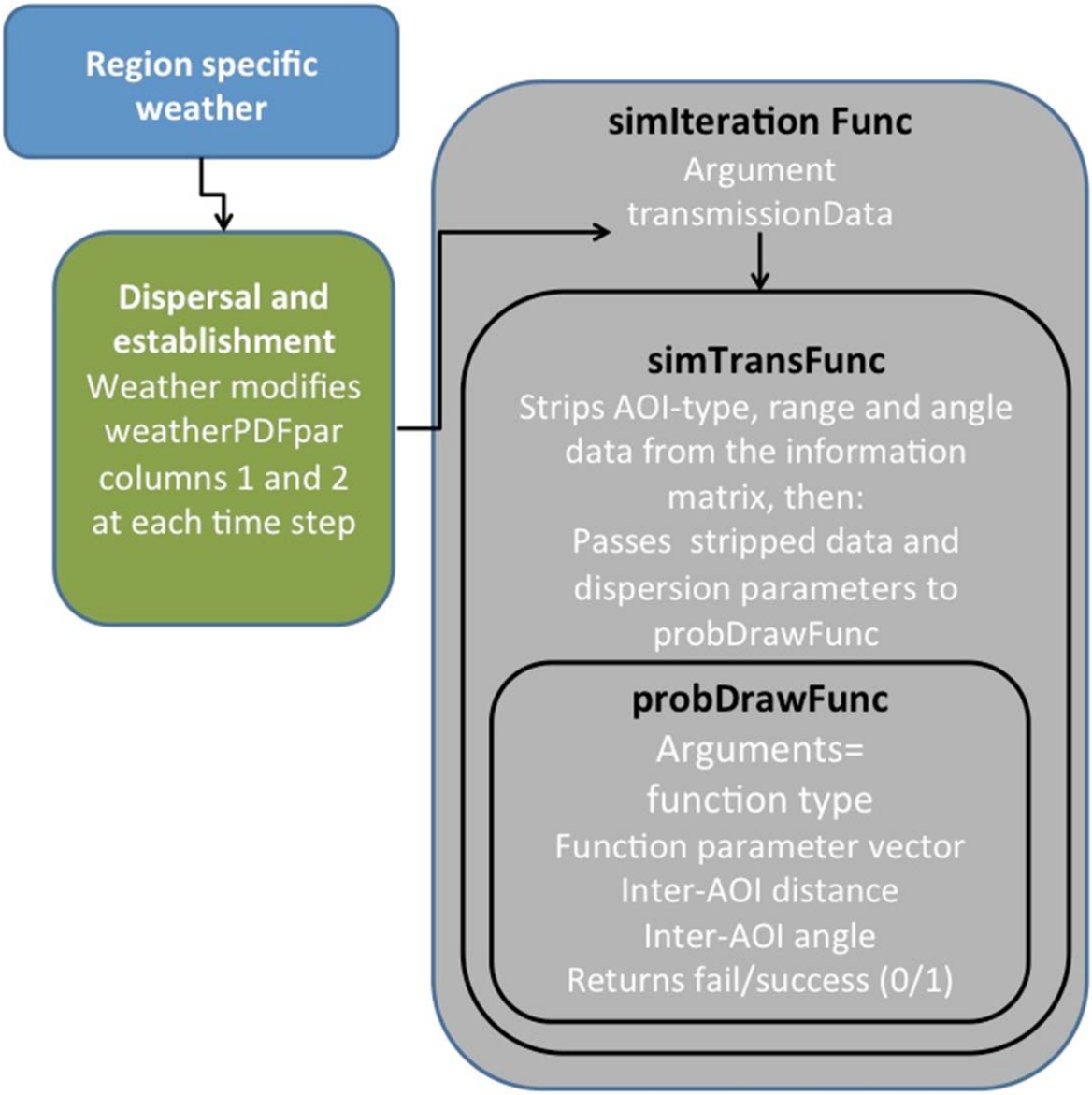

Fig. A3: Model implementation of trials of probability and dispersal Pr(disp). The model structure allows AOI-to-AOI specific time-varying Pr(disp) that are held in the green box (a .csv file) and are currently modified by weather data. Within the main function `simIterationFunc` a wrapper function `simTransFunc` is called to handled data from the

information matrix and pass the data to the `probDrawFunc`, where Bernoulli trials are performed.

The model is implemented so that after the initial probability matrices are created, Pr(disp) are only recalculated when changes are made to the dispersion and establishment parameters (green box; Figure A3).

10.2. Candidate dispersal and establishment functions

Dispersal and establishment functions are coded within the `probDrawFunc` function. Dispersal and establishment mechanisms can be modelled using a variety of functional forms. The current model implementation can accommodate functional forms requiring up to three parameters. The model is implemented to allow the user considerable flexibility when specifying dispersal and establishment functions. The user can: (1) implement AOI-type to AOI-type specific dispersal and functions, and (2) varying the dispersal and function parameters at each time step. For example, in the citrus canker model set-up, the dispersal and establishment pathway "machinery" is modelled by a half-normal function across all AOI types, but this could be changed to AOI-type specific function or parameters. Users can select from the following coded functions are:

Dispersal and establishment function	Number of parameters	Description
Bernoulli (BERN)	1	Distance independent
Half-normal (HNORM)	1	Distance dependent
Hazard rate (HAZARDRATE)	2	Distance dependent
Logistic (LOGISTIC)	2	Distance dependent
North American Animal Disease Spread Model (NAADSM)	2	Based upon mean number of contact events, each with a fixed probability of occurring
Weather (WIND)	2	Based on inter-AOI angle relative to wind direction and inter-AOI distance.

Further functional forms can be added to the `probDrawFunc` R code.